



Siberian Branch of Russian Academy of Science

BUDKER INSTITUTE OF NUCLEAR PHYSICS

F.13  
1999

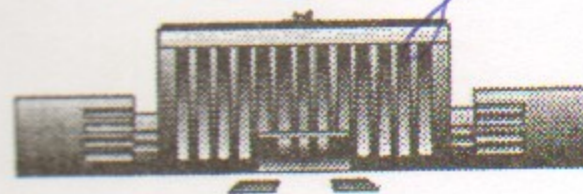
V.S. Fadin and A.D. Martin

INFRARED SAFETY  
OF IMPACT FACTORS FOR COLOURLESS  
PARTICLE INTERACTION

Budker INP 99-38

<http://www.inp.nsk.su/publications>

БИБЛИОТЕКА  
Института ядерной  
Физики СО АН СССР  
ИНВ. № 122



Novosibirsk  
1999



Siberian Branch of Russian Academy of Science

BUDKER INSTITUTE OF NUCLEAR PHYSICS

V.S. Fadin and A.D. Martin

INFRARED SAFETY OF IMPACT FACTORS  
FOR COLOURLESS PARTICLE  
INTERACTION

Budker INP 99-38

Novosibirsk

1999



V.S. Fadin and A.D. Martin<sup>a</sup>

Budker Institute of Nuclear Physics  
and Novosibirsk State University  
630090 Novosibirsk, Russia

<sup>a</sup> Department of Physics, University of Durham,  
Durham, DH1 3LE

### Abstract

We demonstrate, to next-to-leading order accuracy, the cancellation of the infrared singularities in the impact factors which arise in the QCD description of high energy processes  $A+B \rightarrow A'+B'$  of colourless particles. We study the example where  $A$  is a virtual photon in detail, but show that the result is true in general.

## 1 Introduction

There continues to be much activity in the study of semihard QCD processes, that is processes at small values of  $x = Q^2/s$  where  $Q^2$  is a typical virtuality and  $\sqrt{s}$  is the centre-of-mass energy. Many intriguing low  $x$  phenomena have been observed (see, for example, ref. [1]) since the announcement of the sharp rise seen in the proton structure function at HERA at  $x$  decreases. The theoretical understanding of these phenomena is a non-trivial task. One important type of process is high energy diffractive  $q\bar{q}$  (or vector meson) electroproduction, which to lowest order proceeds via two gluon exchange. Much data are becoming available for such reactions. However the size of the QCD radiative corrections is not known. There are indications both experimentally and phenomenologically that these corrections are very important [2]. Another relevant process is the total cross section for  $\gamma^*\gamma^*$  collisions.

The most common basis for the description of small  $x$  processes is the BFKL equation [3]. In this approach the amplitude for the high energy process  $A+B \rightarrow A'+B'$  at fixed momentum transfer  $\sqrt{-t}$  may be symbolically written as the convolution

$$\Phi_{A'A} \otimes G \otimes \Phi_{B'B}, \quad (1)$$

see Fig. 1 and eq.(2) below. The impact factors  $\Phi_{A'A}$  and  $\Phi_{B'B}$  describe the transitions  $A \rightarrow A'$  and  $B \rightarrow B'$  shown by the upper and lower blobs of Fig. 1, while  $G$  is the Green's function for the two interacting Reggized gluons. This representation is valid both in the leading logarithmic approximation (LLA) [3], when only the leading terms  $(\alpha_S \ln s)^n$  are resummed, and in the next-to-leading approximation (NLA) [4, 5], when the  $\alpha_S(\alpha_S \ln s)^n$  terms are also resummed, not only for forward scattering [4, 5] with  $t = 0$ , but for the non-forward case [6] as well. The explicit form of the kernel for forward scattering (with colourless exchange in the  $t$  channel) was found in ref. [4, 5]. A number of subsequent papers (see, for instance, [7]) were devoted to investigations of its consequences.



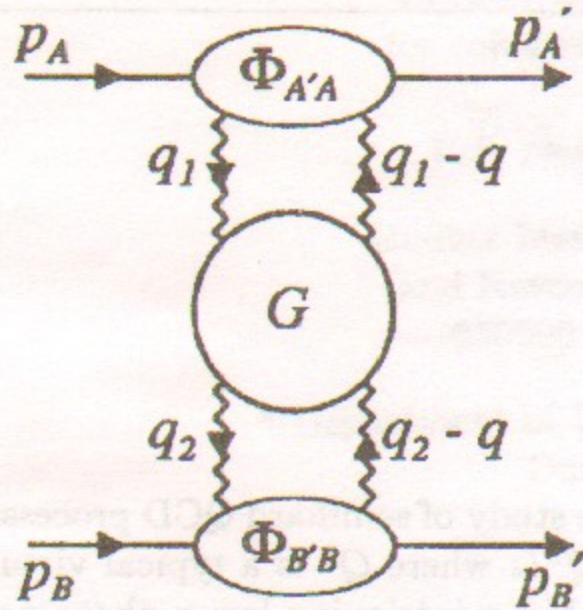


Figure 1: Schematic representation of the process  $A + B \rightarrow A' + B'$  displaying the structure of (2). The zig-zag lines represent Reggeized gluon exchange.

Both the kernel of the integral equation satisfied by the Green's function and the impact factors are unambiguously defined [4, 6, 8] in terms of the gluon Regge trajectory and the effective vertices for the Reggeon-particle interactions, which have been calculated in the NLA in a series of papers [9]-[12].<sup>1</sup> The cancellation of the infrared singularities in the kernel was explicitly demonstrated in ref. [4]. We stress that, for brevity, we are using the terminology "infrared singularities" to include both soft and collinear singularities. Strictly speaking the Green's function for the Reggeized gluons, taken by itself, is not physical, since only the amplitudes describing the interaction of colourless particles are measurable. It is these physical amplitudes that must be free of infrared singularities. However since it has been shown that the kernel of the equation for the Green's function is infrared safe, it should therefore be possible to construct impact factors which are infrared safe. Recall that we are discussing impact factors for transitions between colourless particles and, consequently, about a colour singlet state in the  $t$  channel.

Here we study such impact factors at NLA accuracy. We demonstrate explicitly the cancellation of the infrared singularities in the impact factor of the virtual photon and, moreover, give a proof that the impact factors describing the transitions between colourless particles are infrared safe in general. We concentrate on the virtual photon because of the importance of the NLA for diffractive  $q\bar{q}$  electroproduction, as mentioned above. Our study may therefore be considered as a first step in analyzing the next-to-leading radiative corrections to this experimentally accessible process.

<sup>1</sup>The impact factors were defined in refs. [5, 13, 14] in a different way; see the comment in Section 7.

The outline of the paper is as follows. In Section 2 we give a detailed definition of the impact factor, concentrating on the example of that for a virtual photon. In Section 3 we calculate the singular contribution which comes from the *virtual* correction to the LLA approximation for the effective virtual photon-Reggeon interaction. Then in Section 4 we consider the effects arising from an additional *real* gluon emitted in the  $\gamma^*$ -Reggeon interaction. In Section 5 we draw these results together and demonstrate the cancellation of the infrared singularities in the impact factor of the virtual photon in the NLA. A proof of the cancellation in the general case is given in Section 6. Finally, in Section 7 we present our conclusions.

## 2 The definition of the impact factors

First we make explicit the convolution (1) for the amplitude  $T$  describing the process  $A + B \rightarrow A' + B'$  shown in Fig. 1. To be specific we calculate the  $s$ -channel imaginary part of the amplitude [6]

$$\text{Im}T = \int \frac{d^{D-2}q_1}{q_1^2 q_1'^2} \int \frac{d^{D-2}q_2}{q_2^2 q_2'^2} \Phi_{A'A}(q_1, q; s_0) \times \frac{s}{(2\pi)^{D-2}} \int_{\delta-i\infty}^{\delta+i\infty} \frac{d\omega}{2\pi i} \left[ \left( \frac{s}{s_0} \right)^\omega G_\omega(q_1, q_2; q) \right] \Phi_{B'B}(-q_2, -q; s_0), \quad (2)$$

where the momenta are defined in Fig. 1. For convenience we introduce  $q'_i \equiv q_i - q$ , where  $q \simeq q_T$  is the momentum transfer in the process  $A + B \rightarrow A' + B'$

$$q = p_A - p_{A'} = p_{B'} - p_B. \quad (3)$$

$\Phi_{A'A}$  and  $\Phi_{B'B}$  are the impact factors which describe the  $A \rightarrow A'$  and  $B \rightarrow B'$  particle transitions in the particle-Reggeon scattering processes shown in Fig. 1, and  $G_\omega$  is the Mellin transform of the Green's function for Reggeon-Reggeon scattering. We emphasize that the zig-zag intermediate lines in Fig. 1 denote Reggeons, and not gluons — the Reggeons would only become gluons in the absence of interaction. The integrations in (2) are performed over  $D - 2$  dimensional vectors which are transverse to the momenta  $p_A$  and  $p_B$  of the initial particles. The space-time dimension,  $D$ , is taken to be  $D = 4 + 2\epsilon$  in order to regularize the infrared divergences.

Representation (2) is derived assuming that the energy scale  $s_0$  is independent of  $q_1$  and  $q_2$ , or at least has a factorizable dependence on  $q_1$  and  $q_2$ . Then any  $s_0$  dependence induced by using  $s_0$  as the energy scale in  $G_\omega$  can, to NLA accuracy, be transferred to the impact factors. This was



shown in ref. [15] for forward scattering; for the non-forward case the proof is essentially unchanged.

We consider a colour singlet state in the  $t$ -channel (or, to be more precise, vacuum or Pomeron quantum number exchange), since only in this case will the infrared singularities cancel. Thus we can suppress the colour group representation indices of the impact factors and the Green's function. We also note that representation (2) applies not only to elastic processes, but also to reactions where  $A'$  and  $B'$  may each correspond to a group of particles with invariant mass independent of  $s$ . Finally the normalisation adopted in (2) is that of [6], which seems to be convenient for non-forward processes. It differs at  $t = 0$  from that used previously such that

$$G_\omega(\mathbf{q}_1, \mathbf{q}_2; \mathbf{q})|_{q=0} = q_1^2 q_2^2 G_\omega(\mathbf{q}_1, \mathbf{q}_2), \quad (4)$$

where  $G_\omega(\mathbf{q}_1, \mathbf{q}_2)$  is the Mellin transform that was used for the forward case [4].

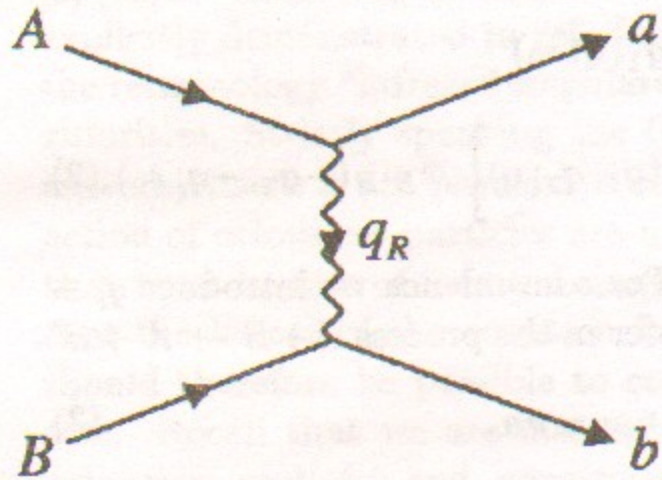


Figure 2: The intermediate process  $A + B \rightarrow a + b$  mediated by Reggeized gluon exchange.

We may express both the kernel of the equation for the Green's function and the impact factors in terms of the gluon Regge trajectory and the effective vertices for the Reggeon-particle interaction [6]. We begin with the high energy amplitude  $T^{(8)}$  for the process  $A + B \rightarrow a + b$  of Fig. 2, which is an intermediate process of our reaction  $A + B \rightarrow A' + B'$ . We have colour octet Reggeized gluon exchange in the  $t_R$  channel ( $t_R = q_R^2 \simeq q^2$ ) with negative signature so that

$$T^{(8)} = \frac{2s}{t_R} \Gamma_{aA}^i(q_R) \left[ \frac{1}{2} \left( \frac{-s}{-t_R} \right)^{\omega(t_R)} + \frac{1}{2} \left( \frac{s}{-t_R} \right)^{\omega(t_R)} \right] \Gamma_{bB}^i(-q_R), \quad (5)$$

where  $\Gamma_{aA}^i$  and  $\Gamma_{bB}^i$  are the Reggeon vertices for transitions  $A \rightarrow a$  and  $B \rightarrow b$  and  $1 + \omega(t)$  is the gluon Regge trajectory. Note that this representation

is true for particle-parton as well as for parton-parton processes. By parton we mean a coloured quark or gluon, whereas a particle is colourless. In the parton-parton case the vertices are known in the one-loop approximation [10]. One of our aims is to identify the particle-parton vertices in the same approximation. The trajectory function,

$$j(t) = 1 + \omega(t), \quad (6)$$

is independent of the nature of the scattering objects, and is now known in the two-loop approximation [11]. The summation over the repeated index  $i$  is over the 8 coloured gluon states.

In the LLA the impact factors are given by

$$\Phi_{A'A}^{(0)}(q_R, q) = \frac{1}{\sqrt{N_C^2 - 1}} \sum_{\{a\}} \int \frac{dM_a^2}{2\pi} \Gamma_{aA}^{(0)i}(q_R) \Gamma_{aA'}^{(0)i}(q_R)^* d\rho_a, \quad (7)$$

where the number of colours  $N_C = 3$  for QCD and  $\Gamma^{(0)}$  means that the vertices are evaluated in the LLA or Born approximation. The sum  $\{a\}$  is over all states  $a$  which contribute to the  $A \rightarrow A'$  transition, and over all discrete quantum numbers of these states. The phase space element  $d\rho_a$  of a state  $a$  consisting of particles with momenta  $\ell_n$  is

$$d\rho_a = (2\pi)^D \delta \left( p_A - q_R - \sum_{n \in a} \ell_n \right) \prod_{n \in a} \frac{d^{D-1} \ell_n}{(2\pi)^{D-1} 2E_n}, \quad (8)$$

while the remaining integration in (7) is over the squared invariant mass of the state  $a$

$$M_a^2 = (p_A - q_R)^2 = (p'_A - q'_R)^2.$$

In the LLA the impact factors do not depend on  $s_0$ . In fact the energy scale is arbitrary in this approximation.

To be specific, we choose the relevant example of the impact factor of a virtual photon  $\gamma^*$ . In order to define the vertices  $\Gamma_{a\gamma^*}^i$  we may study the high energy interaction of the  $\gamma^*$  with any particle. Clearly we should take the simplest choice for particle  $B$  — a massless quark with momentum  $p_B = p_2$  and  $p_2^2 = 0$  — and introduce the light-cone momentum  $p_1$  so that the virtual photon momentum is

$$p_A = p_1 - \frac{Q^2}{s} p_2 \quad \text{and} \quad s = 2p_1 \cdot p_2, \quad (9)$$

where  $-Q^2$  is the virtuality of the photon.



The lowest-order  $\gamma^* q$  process which has a non-vanishing cross section at large  $s$  is  $\gamma^* q \rightarrow (q\bar{q})q$  where the  $q\bar{q}$  pair is produced in the fragmentation region of the photon. The Feynman diagrams are shown in Fig. 3. We may evaluate these diagrams using the trick of writing the metric tensor in the gluon propagator as

$$g^{\mu\nu} = \frac{2p_2^\mu p_1^\nu}{s} + \frac{2p_1^\mu p_2^\nu}{s} + g_{\perp}^{\mu\nu}, \quad (10)$$

and retaining just the first term. Only this term gives a leading (growing as  $s$ ) contribution to the amplitude. In this way we arrive at the  $\gamma^* q \rightarrow (q\bar{q})q$  Born amplitude in the form of (5) with the lower vertex (describing the  $q \rightarrow q'$  transition via the Reggeon field) given by

$$\Gamma_{q',q}^{(0)i} = g\bar{u}(p_2') \frac{\not{p}_1}{s} t^i u(p_2) = g\langle q'|t^i|q\rangle \delta_{\lambda_2\lambda_2'} \quad (11)$$

and the upper vertex (describing the  $\gamma^* \rightarrow q\bar{q}$  transition) given by

$$\Gamma_{q\bar{q},\gamma^*}^{(0)i}(q_R) = \langle q|t^i|\bar{q}\rangle \Gamma_{q\bar{q},\gamma^*}(q_R); \quad \Gamma_{q\bar{q},\gamma^*}(q_R) = \Gamma_a + \Gamma_b \quad (12)$$

with

$$\Gamma_a = \frac{ee_q g}{s} \bar{u}(l_+) \frac{\not{\epsilon}_{\gamma^*}(\not{l}_- + \not{q}_R)\not{p}_2}{\Delta_-} v(l_-) \quad (13)$$

$$\Gamma_b = -\frac{ee_q g}{s} \bar{u}(l_+) \frac{\not{p}_2(\not{l}_+ + \not{q}_R)\not{\epsilon}_{\gamma^*}}{\Delta_+} v(l_-). \quad (14)$$

The components  $\Gamma_a$  and  $\Gamma_b$  correspond to the upper vertices in diagrams 3a and 3b respectively. The notation used in (11)–(14) is as follows:  $\lambda$  denotes the quark helicity,  $g$  is the QCD coupling and  $\langle a|t^i|b\rangle$  are the matrix elements of the colour generator in the fundamental representation. Also  $ee_q$  is the electric charge of the quark (in the  $q\bar{q}$  pair),  $\epsilon_{\gamma^*}$  is the polarization vector of the photon,  $l_{\pm}$  are the  $q$  and  $\bar{q}$  momenta shown in Fig. 3 and, finally,

$$\Delta_{\pm} = \frac{\ell_{\pm}^2}{x_{\pm}} + x_{\pm} Q^2. \quad (15)$$

We have taken the quark to be massless and have used the decomposition

$$l_{\pm} = x_{\pm} p_1 + \frac{\ell_{\pm}^2}{sx_{\pm}} p_2 + l_{\pm\perp}, \quad \ell_{\pm}^2 \equiv -\ell_{\pm\perp}^2. \quad (16)$$

In fact the expressions (11)–(14) for the vertices could have been written immediately by noting that the vertex factors<sup>2</sup>  $igt^i \not{p}_{1,2}/s$  describe the interaction of a Reggeon with quarks having a large component of momentum along  $p_{2,1}$  respectively. In other words in the LLA the Reggeon acts as gluon with polarization vector  $-p_{2,1}/s$  when it interacts with a quark having a large component of momentum along  $p_{1,2}$  respectively. Taking this into account we can represent the vertices  $\Gamma_{q\bar{q},\gamma^*}^{(0)i}$  by the diagrams of Fig. 4.

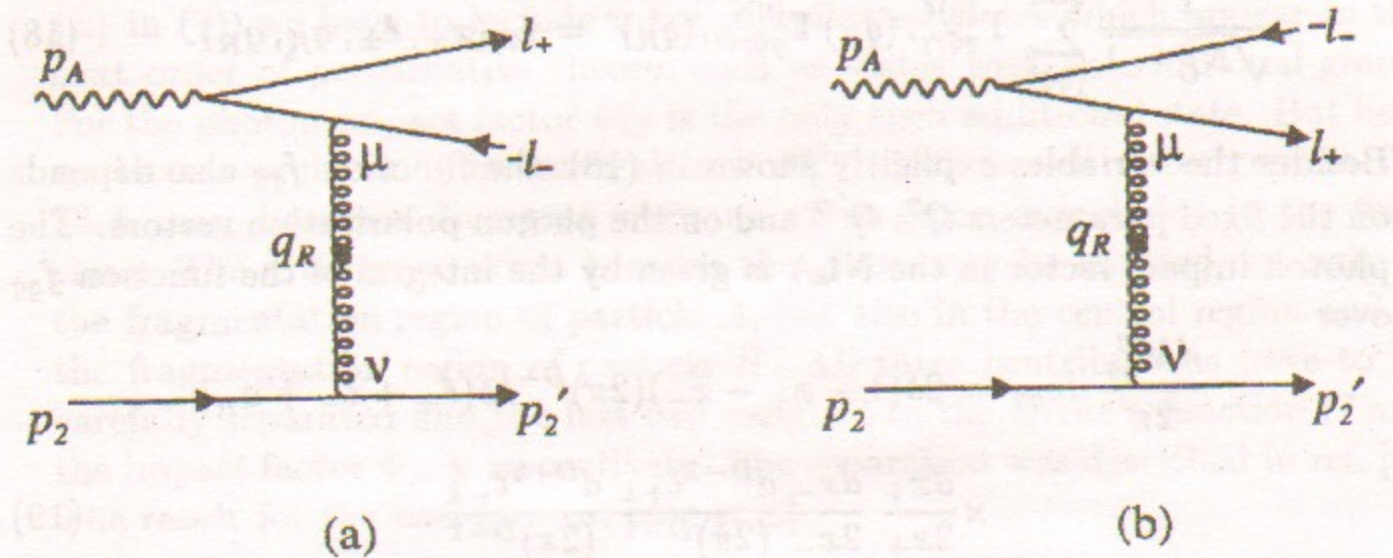


Figure 3: The lowest-order Feynman diagrams for the process  $\gamma^* q \rightarrow (q\bar{q})q$ , showing the particle four momenta.

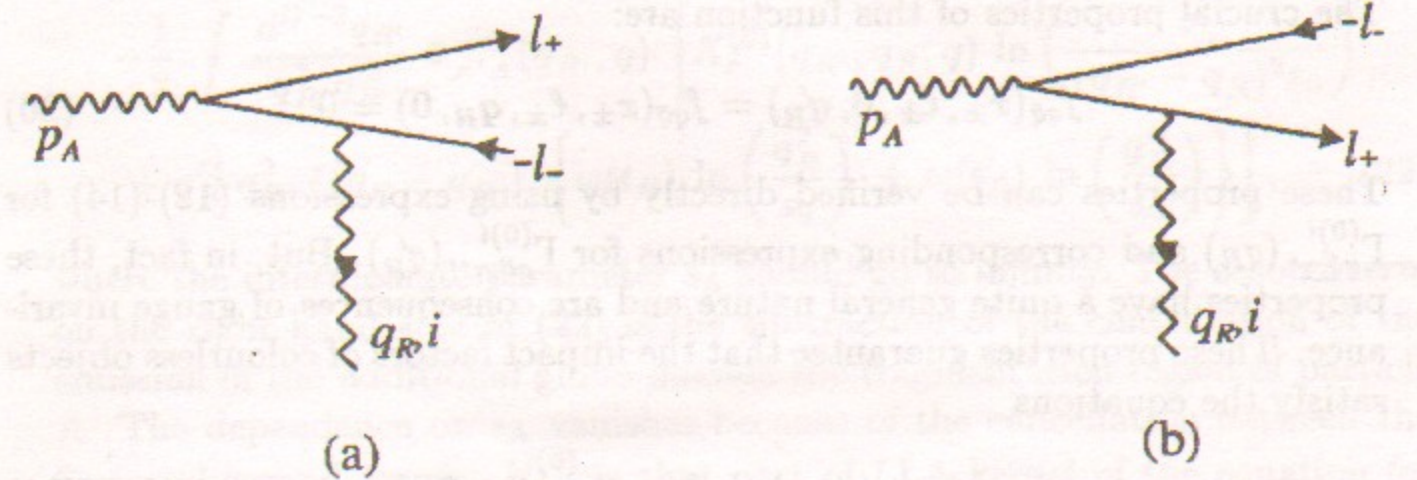


Figure 4: Schematic representation of the vertex  $\Gamma_{q\bar{q},\gamma^*}^{(0)i}$ , showing, at lowest order, the transition  $\gamma^* R \rightarrow q\bar{q}$ .

The vertex  $\Gamma_{q\bar{q},\gamma^*}^{(0)i}(q_R')$  can be calculated in just the same way. It is given

<sup>2</sup>These are the simplest vertices in the effective action for Reggeon interactions [16] which contains all LLA Reggeon-parton vertices.



by (12)–(14) with replacements  $\gamma^* \rightarrow \gamma'^*$ ,  $q_R \rightarrow q'_R$ ,  $\Delta_{\pm} \rightarrow \Delta'_{\pm}$ , where

$$\Delta'_{\pm} = \frac{(\ell_{\mp} + x_{\mp} q)^2}{x_{\mp}} + x_{\pm} Q'^2 \quad (17)$$

and  $-Q'^2$  is the virtuality of the final photon.

Let us denote

$$\frac{1}{\sqrt{N_C^2 - 1}} \sum_{\{q\bar{q}\}} \Gamma_{q\bar{q};\gamma^*}^{(0)i}(q_R) \Gamma_{q\bar{q};\gamma'^*}^{(0)i}(q'_R)^* = f_{q\bar{q}}(x_{\pm}, \ell_{\pm}, q_R, q'_R). \quad (18)$$

Besides the variables explicitly shown in (18), the function  $f_{q\bar{q}}$  also depends on the fixed parameters  $Q^2$ ,  $Q'^2$  and on the photon polarisation vectors. The photon impact factor in the NLA is given by the integral of the function  $f_{q\bar{q}}$  over

$$\begin{aligned} \frac{dM_{q\bar{q}}^2}{2\pi} d\rho_{q\bar{q}} &= 2\delta(1 - x_+ - x_-)(2\pi)^{D-1} \delta(\ell_+ + \ell_- + q_R) \\ &\times \frac{dx_+}{2x_+} \frac{dx_-}{2x_-} \frac{d^{D-2}\ell_{+\perp}}{(2\pi)^{D-1}} \frac{d^{D-2}\ell_{-\perp}}{(2\pi)^{D-1}}. \end{aligned} \quad (19)$$

In fact this impact factor differs by only trivial factors from the analogous one in QED, which was obtained for some particular cases many years ago [17]. The explicit form of the function  $f_{q\bar{q}}$  is not important for our purposes. The crucial properties of this function are:

$$f_{q\bar{q}}(x_{\pm}, \ell_{\pm}, 0, q'_R) = f_{q\bar{q}}(x_{\pm}, \ell_{\pm}, q_R, 0) = 0. \quad (20)$$

These properties can be verified directly by using expressions (12)–(14) for  $\Gamma_{q\bar{q};\gamma^*}^{(0)i}(q_R)$  and corresponding expressions for  $\Gamma_{q\bar{q};\gamma'^*}^{(0)i}(q'_R)$ . But, in fact, these properties have a quite general nature and are consequences of gauge invariance. These properties guarantee that the impact factors of colourless objects satisfy the equations

$$\Phi_{A'A}(0, q) = \Phi_{A'A}(q, q) = 0, \quad (21)$$

that are necessary for the corresponding cross sections to be finite.

The next important fact is that the integral of the function  $f_{q\bar{q}}$  over the measure (19) is not singular, so that we can take  $x_{\pm} \sim 1$ ,  $\ell_{\pm}^2 \sim \mu^2$ , with some nonzero  $\mu$  depending on  $Q^2$ ,  $Q'^2$ ,  $q_R^2$ ,  $(q_R - q)^2$ . For our purposes we can consider all these parameters to be of the same order. In the following we use  $\mu^2$  to denote this order.

In the NLA the expression (7) for the impact factor has to be changed in two ways. First we have to take into account the radiative corrections to the vertices  $\Gamma$  considered above. We note that the corrections depend on an energy scale. In the definition (5) the energy scale was put equal to  $-t_R$ . Since we calculate impact factors for scale  $s_0$  we must allow for the change of the vertices arising from the change of scale. It is clear from (5) that the ratio of vertex factors evaluated at scales  $s_1$  and  $s_2$  is equal to  $(s_2/s_1)^{\omega(t_R)/2}$  for a Reggeon of momentum  $q_R$ . Secondly, in the sum over  $\{a\}$  in (7), we have to include more complicated states which appear in the next order of perturbative theory, such as states with an additional gluon. For the photon impact factor  $q\bar{q}g$  is the only such additional state. But here we have a problem. The integral over  $M_a^2$ , which is well convergent in the LLA case, becomes divergent when an extra gluon is included in the final state. The divergence arises because the gluon may be emitted not only in the fragmentation region of particle  $A$ , but also in the central region and in the fragmentation region of particle  $B$ . All three contributions have to be carefully separated and the last two assigned to the Green's function  $G$  and the impact factor  $\Phi_{B'B}$  respectively. The separation was described in ref. [8]. The result for the non-forward case is [6]

$$\begin{aligned} \Phi_{A'A}(q_R, q; s_0) &= \frac{1}{\sqrt{N_C^2 - 1}} \sum_{\{a\}} \int \frac{dM_a^2}{2\pi} \Gamma_{aA}^i(q_R) \Gamma_{aA'}^i(q'_R)^* d\rho_a \theta(s_A - M_a^2) \\ &- \frac{1}{2} \int \frac{d^{D-2}q_{R'}}{q_{R'}^2 q_{R'}'^2} \Phi_{A'A}^{(0)}(q_{R'}, q) \left[ K_r^{(0)}(q_{R'}, q_R; q) \ln \left( \frac{s_A^2}{(q_{R'} - q_R)^2 s_0} \right) \right. \\ &\left. + q_{R'}'^2 q_R'^2 \delta(q_R - q_{R'}) \left\{ \omega(t_R) \ln \left( \frac{q_R'^2}{s_0} \right) + \omega(t'_R) \ln \left( \frac{q_{R'}'^2}{s_0} \right) \right\} \right], \end{aligned} \quad (22)$$

where the intermediate parameter  $s_A$  should go to infinity. The second term on the right hand side of (22) is the subtraction of the contribution of the emission of the additional gluon outside the fragmentation region of particle  $A$ . The dependence on  $s_A$  vanishes because of the cancellation between the first and second terms.  $K_r^{(0)}$  is that part of LLA kernel of the equation for the non-forward Green's function which is related to real gluon production [3]

$$K_r^{(0)}(q_{R'}, q_R; q) = \frac{g^2 N_C}{(2\pi)^{D-1}} \left( \frac{q_{R'}^2 q_{R'}'^2 + q_R'^2 q_R'^2}{(q_R - q_{R'})^2} - q^2 \right). \quad (23)$$

The kernel describes the transition from the  $t$  channel state of two Reggeons with momenta  $q_R$  and  $-q'_R \equiv q - q_R$  into the state with  $q_{R'}$  and  $-q'_{R'} \equiv q - q_{R'}$ .



The terms which involve the Regge trajectory in (22) arise from the change of energy scale in the vertices  $\Gamma$ . The trajectory function  $\omega(t)$  has to be taken in the one loop approximation [3]

$$\omega(t) = \frac{g^2 t}{(2\pi)^{D-1}} \frac{N_C}{2} \int \frac{d^{D-2}k}{k^2(q-k)^2} = -\bar{g}^2(q^2)^\epsilon \frac{\Gamma^2(\epsilon)}{\Gamma(2\epsilon)}, \quad (24)$$

where  $\Gamma(x)$  is the Euler function and

$$\bar{g}^2 \equiv g^2 N_C \Gamma(1-\epsilon)/(4\pi)^{D/2}. \quad (25)$$

As stated above, to evaluate the photon impact factor in NLA we have to evaluate the virtual corrections to the  $\gamma^* \rightarrow q\bar{q}$  vertex of (12) and to include the effects of the emission of an additional gluon (that is to find the  $\gamma^* \rightarrow q\bar{q}g$  vertices and to include their contribution in (22)). We begin with the virtual corrections.

### 3 One-loop corrections to the $\gamma^* R \rightarrow q\bar{q}$ vertex

One way to determine the corrections to the  $\gamma^* R \rightarrow q\bar{q}$  vertex is to calculate the one-loop corrections to the diagrams of Fig. 3 with a colour-octet state in the  $t_R$  channel. We keep not only the  $\ln s$  terms, but the constant terms as well. We will find the coefficient of the  $\ln s$  term, which is due to gluon Reggeization, is

$$\frac{2s}{t_R} \Gamma_{q\bar{q},\gamma^*}^{(0)i} \Gamma_{q',q}^{(0)i} \omega(t_R) \quad (26)$$

as it must be. If we compare the calculated corrected amplitude with representation (5) and use the known<sup>3</sup> expression for the lower vertex  $\Gamma_{q',q}^i$  to one-loop accuracy [10], then we may extract  $\Gamma_{q\bar{q},\gamma^*}^i$  in the one-loop approximation.

In practice we can determine the  $\gamma^* R \rightarrow q\bar{q}$  vertex to one-loop accuracy in a more economical way by focusing attention directly on the vertex and not on the amplitude. To be specific we work in the Feynman gauge. There are several ways in which we can add the extra virtual gluon line to the diagrams of Fig. 3. It is clear that if one end of the extra gluon line is attached to the  $q$  or  $\bar{q}$  of the upper  $q\bar{q}$  pair and the other end is either again attached to one of the upper pair or to the exchanged gluon, then the correction is to the upper vertex. Similar considerations apply to the lower vertex. It is

<sup>3</sup>It was determined using the same procedure for the quark-quark scattering process.

also clear that half the gluon self-energy correction has to be included in the upper vertex and half in the lower vertex. The only uncertainty comes from the diagrams of Fig. 5 with two gluon lines exchanged between the upper and the lower vertices. Perhaps a better terminology, which we shall adopt, is to say two gluons exchanged between the upper and lower blocks. We analyse these two-gluon exchange diagrams first.

### 3.1 Two-gluon exchange diagrams

We start with diagram 5(a). The basic integral for this diagram is

$$I_{5a} = \int \frac{d^D k}{(2\pi)^D i} \frac{1}{(k^2 + i0)((q_R - k)^2 + i0)((p'_2 - k)^2 + i0)((\ell_- + k)^2 + i0)}. \quad (27)$$

It is convenient to use the Sudakov decomposition for the gluon momentum,

$$k = \beta p_1 + \alpha p_2 + k_\perp, \quad d^D k = \frac{s}{2} d\alpha d\beta dk_\perp^{D-2}, \quad (28)$$

and to consider three regions of the variables  $\alpha, \beta$ :

$$\begin{array}{ll} \text{the central region} & |\alpha| < \alpha_0, \quad |\beta| < \beta_0 \\ \text{the } A \text{ region} & |\beta| \geq \beta_0 \\ \text{the } B \text{ region} & |\alpha| \geq \alpha_0, \end{array} \quad (29)$$

with  $\alpha_0$  and  $\beta_0$  chosen so that

$$\alpha_0 \ll 1, \quad \beta_0 \ll 1 \quad \text{and} \quad s\alpha_0\beta_0 \gg \mu^2. \quad (30)$$

Recall that we use  $\mu$  to denote the order of magnitude of typical transverse momenta. In fact we will take the limit  $s\alpha_0\beta_0 \rightarrow \infty$ , while  $\alpha_0 \rightarrow 0$  and  $\beta_0 \rightarrow 0$ . We see that regions  $A$  and  $B$  overlap. The whole  $\alpha, \beta$  plane is covered by the sum of the three regions, with the subtraction of the overlapping subregions where both of the variables are "large", that is  $|\alpha| > \alpha_0$  and  $|\beta| > \beta_0$ . If we decompose the momentum transfer

$$q_R = \beta R p_1 + \alpha R p_2 + q_{R\perp} \quad (31)$$

then we have

$$s\beta_R \simeq q_{R\perp}^2, \quad s\alpha_R \simeq -Q^2 - \frac{\ell_-^2}{x_-} - \frac{\ell_+^2}{x_+}. \quad (32)$$



Combining this with the fact that all transverse momenta are of order  $\mu$ , it is easy to show that the overlapping regions where  $|\alpha|$  and  $|\beta|$  are both "large" give a contribution of relative order  $\lesssim \mu^2/s\alpha_0\beta_0$ , which vanishes in the limit  $s \rightarrow \infty$ . Thus  $I_{5a}$  is given by the sum of the contributions from the three regions. The result for the central region ( $|\alpha| < \alpha_0, |\beta| < \beta_0$ ) is

$$I_{5a}^{\text{central}} = \frac{2\Gamma(1-\epsilon)}{(4\pi)^{D/2}} \frac{\Gamma^2(\epsilon)}{\Gamma(2\epsilon)} \frac{(q_R^2)^{\epsilon-1}}{2sx_-} \quad (33)$$

$$\times \left[ -\ln\left(\frac{-s\alpha_0\beta_0}{q_R^2}\right) + \psi(1) - \psi(1-\epsilon) + 2\psi(\epsilon) - 2\psi(2\epsilon) \right],$$

where  $\psi(x) = \Gamma'(x)/\Gamma(x)$ . We emphasize the important fact that the contribution of the central region is universal (i.e. process independent). The above equation gives not only the singular  $1/\epsilon$  term, but also the general  $\epsilon$  dependence. For completeness we give the contributions from regions A and B which are non-vanishing as  $\epsilon \rightarrow 0$ :

$$I_{5a}^A = \frac{2\Gamma(1-\epsilon)}{(4\pi)^{D/2}} \frac{(q_R^2)^{\epsilon-1}}{2sx_-} \left[ -\frac{\Gamma^2(\epsilon)}{\Gamma(2\epsilon)} \ln\left(\frac{x_-}{\beta_0}\right) + \frac{1}{\epsilon^2} + \frac{2}{\epsilon} \ln\left(\frac{\Delta_-}{q_R^2}\right) + \frac{1}{2} \ln^2\left(\frac{\Delta_-}{q_R^2}\right) + L\left(1 - \frac{q_R^2}{\Delta_-}\right) - L\left(1 - \frac{\Delta_-}{q_R^2}\right) + \frac{\pi^2}{6} \right], \quad (34)$$

where

$$L(x) = \int_0^x \frac{dt}{t} \ln(1-t),$$

and

$$I_{5a}^B = \frac{2\Gamma(1-\epsilon)}{(4\pi)^{D/2}} \frac{\Gamma^2(\epsilon)}{\Gamma(2\epsilon)} \frac{(q_R^2)^{\epsilon-1}}{2sx_-} \left[ -\ln\left(\frac{1}{\beta_0}\right) - \psi(1) + \psi(2\epsilon) \right]. \quad (35)$$

We checked by an independent calculation of the integral of (27), using Feynman parameters, that  $I_{5a}$  is indeed given by the sum of the three contributions, and hence that there is a negligible contribution from the regions where both  $|\alpha|$  and  $|\beta|$  are "large".

We now study how the basic integral (27) enters the matrix element. We use the same trick that we used before for the metric tensors in the gluon propagators, see (10). In this way we find factors

$$\not{p}_2(-\not{\ell}_- - \not{k})\not{p}_2 \quad \text{and} \quad \not{p}_1(\not{p}'_2 - \not{k})\not{p}_1 \quad (36)$$

respectively in the numerator for the upper and lower blocks in Fig. 5a. It is clear that we can neglect  $\not{k}$  in the central region. Since we can omit the contribution from the region where both  $|\alpha|$  and  $|\beta|$  are large, we are also able to neglect  $\not{k}$  in the numerator of the upper (lower) block in the A(B) region. We can then factorize from the numerator the corresponding term which arises in the amplitude of Fig. 3a. To see this we use the anticommutation relations of the  $\gamma$  matrices to move  $\not{\ell}_-(\not{p}'_2)$  to act on the spinor  $v(\ell_-)(\bar{u}(p'_2))$ , and then use the Dirac equation. We also have factorization in colour space. We require negative-signature colour-octet exchange in the  $t_R$  channel, and so we need the antisymmetric colour-octet projection of the two-gluon state. The colour structure is thus identical to that of the diagrams of Fig. 3.

Therefore it turns out that the contribution of the "central" region of Fig. 5a to the  $\gamma^*q \rightarrow (q\bar{q})q$  amplitude  $T^{(8)}$  of (5) is

$$T_{5a}^{\text{central}} = \frac{s}{t_R} \langle q|t^i|\bar{q} \rangle \Gamma_a \Gamma_{q',q}^{(0)i} \omega(t_R) \left[ \ln\left(\frac{-s}{q_R^2}\right) + \phi(\alpha_0) + \phi(\beta_0) \right], \quad (37)$$

where  $\Gamma_a$  is the  $\gamma^* \rightarrow q\bar{q}$  Reggeon vertex of (13),  $\Gamma_{q',q}^{(0)i}$  is the  $q \rightarrow q'$  Reggeon vertex of (11),  $\omega$  is the one-loop contribution to the trajectory function of (25), and the  $\phi$  functions are

$$\phi(z) = \ln z - \frac{1}{2} [(\psi(1) - \psi(1-\epsilon)) - \psi(\epsilon) + \psi(2\epsilon)]. \quad (38)$$

Diagrams 5b, 5a' and 5b' can be computed in exactly the same way. The contribution of the central region of Fig. 5b is given by (37) with the replacement of  $\Gamma_b$  of (14) for  $\Gamma_a$ ; while the contributions of 5a' and 5b' are obtained from those of diagrams 5a and 5b by the replacement  $s \rightarrow -s$  and by changing the overall sign (due to antisymmetry in colour space). Collecting all these four central region contributions together we therefore have

$$T^{\text{central}} = \frac{2s}{t_R} \Gamma_{q\bar{q},\gamma^*}^{(0)i} \Gamma_{q',q}^{(0)i} \omega(t_R) \left[ \frac{1}{2} \ln\left(\frac{-s}{q_R^2}\right) + \frac{1}{2} \ln\left(\frac{s}{q_R^2}\right) + \phi(\alpha_0) + \phi(\beta_0) \right], \quad (39)$$

where we have used (12). We see that the logarithmic part of the contribution coincides with the first term in the expansion of (5) in  $\omega(t_R)$ ; that is, it is responsible for gluon Reggeization. The remaining pieces,  $\phi(\alpha_0)$  and  $\phi(\beta_0)$ , must be included as corrections to the corresponding vertices. The important fact is that contribution (39) of the central region is *universal*. That is this result for  $\gamma^*q \rightarrow (q\bar{q})q$  applies to any process  $A+a \rightarrow B+b$ , as



in Fig. 2, with the same expression in square brackets, provided that we use the corresponding vertices.

We now turn to the  $A$  region ( $|\beta| > \beta_0$ , see (29)). We first consider the combined contribution of the diagrams of Figs. 5a, 5a' and 6a. To evaluate diagram 6a we again use the familiar trick (10) for the metric tensor in the propagator of the gluon with momentum  $q_R$ . In this way we show that we can factor out the vertex  $\Gamma_{q',q}^{(0)i}$ . The same factorization applies to diagrams 5a and 5a' in the  $A$  region. Moreover here we can replace

$$(p'_2 - k)^2 + i0 = -s(\beta - \beta_R)(1 - \alpha - \alpha_R) - (q_R - k)^2 + i0 \rightarrow -s\beta \quad (40)$$

$$(p_2 + k)^2 + i0 = s\beta - k^2 + i0 \rightarrow s\beta.$$

Then taking into account the difference in signs for diagrams 5a and 5a' due to colour antisymmetry, we see that they give equal contributions in the  $A$  region. After the factorization of the common factor  $\Gamma_{q',q}^{(0)i}$  we find that the remainder does not depend on the properties of the lower block (vertex). Thus the sum of the remaining contributions of diagrams 5a, 5a' and 6a must give corrections to the vertex  $\Gamma_{q\bar{q},\gamma^*}$ . Moreover this sum is given by Fig. 7a, where we have introduced the off-mass-shell gluon-gluon-Reggeon vertex of Fig. 8

$$\begin{aligned} \gamma_{iab}^{\mu\nu}(k_1, k_2) = & -\frac{ig}{s} T_{ab}^i \left[ -g^{\mu\nu} p_2 \cdot (k_2 - k_1) - p_2^\mu (2k_1 + k_2)^\nu \right. \\ & \left. + p_2^\nu (2k_2 + k_1)^\mu - 2(k_1 + k_2)^2 \frac{p_2^\mu p_2^\nu}{p_2 \cdot (k_1 - k_2)} \right] \end{aligned} \quad (41)$$

where  $T^i$  are the generators in the adjoint representation in colour space;  $T_{ab}^c = -if_{cab}$ .

In the same way we factor off the lower vertex  $\Gamma_{q',q}^{(0)i}$  from the  $A$  region contributions of diagrams 5b, 5b' and 6b, and find that their sum is given by Fig. 7b. It is also clear that the  $B$  region contributions of diagrams 5a, b, a', b', in which the upper vertex  $\Gamma_{q\bar{q},\gamma^*}^{(0)i}$  has been factored off, will give the corrections to the lower quark-quark-Reggeon vertex  $\Gamma_{q',q}$ . We are, however, not concerned with these latter corrections here.

Now we turn to the remaining two gluon exchange diagrams, 5c, c'. Unlike the previous diagrams here both the produced  $q$  and  $\bar{q}$  interact, and they contribute in quite different regions of the Sudakov parameters  $\alpha$  and  $\beta$ .

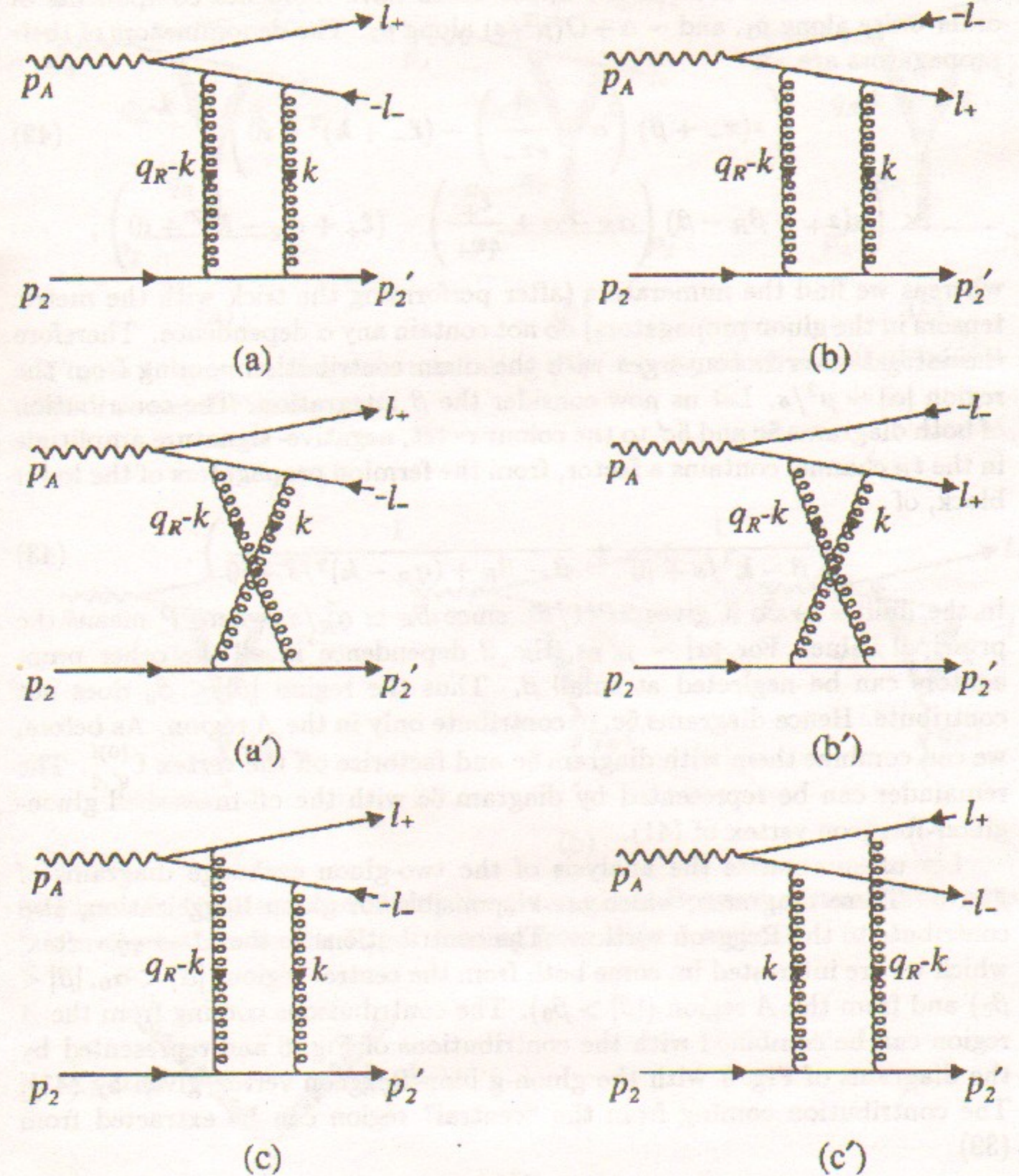


Figure 5: The two-gluon exchange Feynman diagrams mediating the process  $\gamma^* q \rightarrow (q\bar{q})q$ .



Only the region of small  $\alpha$ ,  $|\alpha| \sim \mu^2/s$ , is important. The reason is that the two virtual fermions in the upper block have momenta components of order unity along  $p_1$ , and  $\sim \alpha + O(\mu^2/s)$  along  $p_2$ . The denominators of their propagators are

$$\begin{aligned} & \left( s(x_- + \beta) \left( \alpha + \frac{\ell_-^2}{sx_-} \right) - (\ell_- + k)^2 + i0 \right) \\ & \times \left( s(x_+ + \beta_R - \beta) \left( \alpha_R - \alpha + \frac{\ell_+^2}{sx_+} \right) - (\ell_+ + q_R - k)^2 + i0 \right), \end{aligned} \quad (42)$$

whereas we find the numerators (after performing the trick with the metric tensors in the gluon propagators) do not contain any  $\alpha$  dependence. Therefore the integral over  $\alpha$  converges with the main contribution coming from the region  $|\alpha| \sim \mu^2/s$ . Let us now consider the  $\beta$  integration. The contribution of both diagrams 5c and 5c' to the colour-octet, negative-signature amplitude in the  $t_R$  channel contains a factor, from the fermion propagators of the lower block, of

$$\left( \frac{1}{\beta - k^2/s + i0} + \frac{1}{\beta - \beta_R + (q_R - k)^2/s - i0} \right). \quad (43)$$

In the limit  $s \rightarrow \infty$  it gives  $2P(1/\beta)$ , since  $\beta_R \simeq q_R^2/s$ , where  $P$  means the principal value. For  $|\alpha| \sim \mu^2/s$ , the  $\beta$  dependence in all the other propagators can be neglected at small  $\beta$ . Thus the region  $|\beta| \leq \beta_0$  does not contribute. Hence diagrams 5c, c' contribute only in the  $A$  region. As before, we can combine them with diagram 6c and factorize off the vertex  $\Gamma_{q',q}^{(0)i}$ . The remainder can be represented by diagram 6c with the off-mass-shell gluon-gluon-Reggeon vertex of (41).

Let us summarize the analysis of the two-gluon exchange diagrams of Fig. 5. These diagrams, which are responsible for gluon Reggeization, also contribute to the Reggeon vertices. The contributions to the  $\gamma^* \rightarrow q\bar{q}$  vertex, which we are interested in, come both from the central region ( $|\alpha| < \alpha_0, |\beta| < \beta_0$ ) and from the  $A$  region ( $|\beta| > \beta_0$ ). The contributions coming from the  $A$  region can be combined with the contributions of Fig. 6 and represented by the diagrams of Fig. 7 with the gluon-gluon-Reggeon vertex given by (41). The contribution coming from the "central" region can be extracted from (39)

$$\Delta \Gamma_{q\bar{q},\gamma^*}^{i(\text{central})} = -\bar{g}^2 \frac{\Gamma^2(\epsilon)}{\Gamma(2\epsilon)} (q_R^2)^\epsilon \Gamma_{q\bar{q},\gamma^*}^{(0)i} \phi(\beta_0), \quad (44)$$

where we have used (24), and where  $\phi(z)$  is given by (38). The intermediate parameter  $\beta_0$  cancels when we combine (44) with the contributions of Figs. 7a,b. (The contribution of diagram 7c does not depend on  $\beta_0$ .)

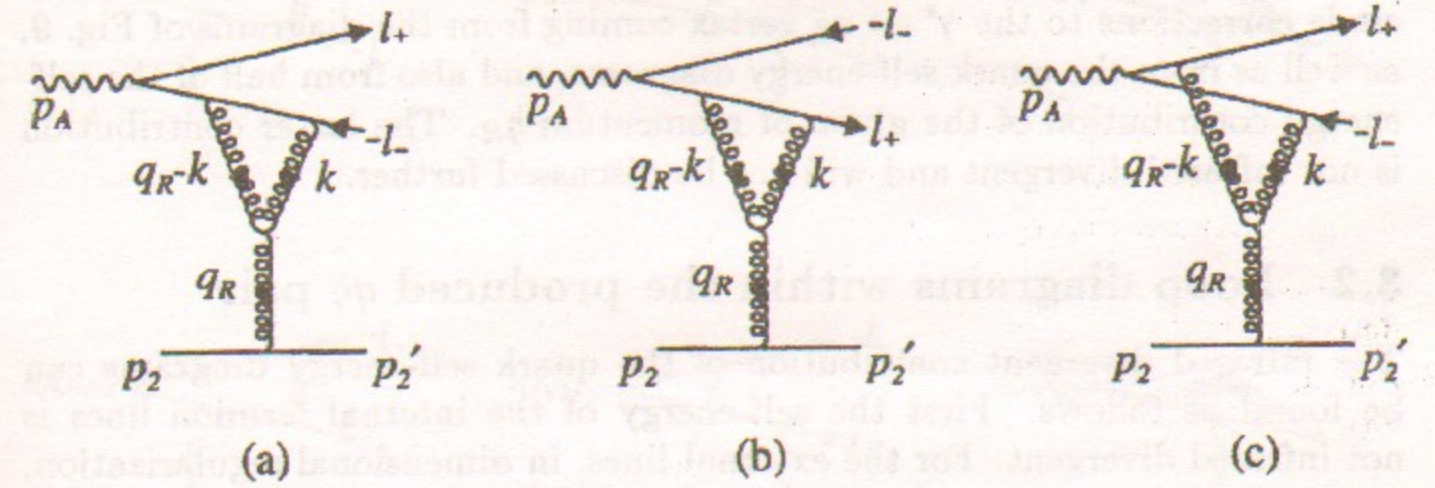


Figure 6: Eynman diagrams mediating  $\gamma^* q \rightarrow (q\bar{q})q$  which must be considered with those of Fig. 5.

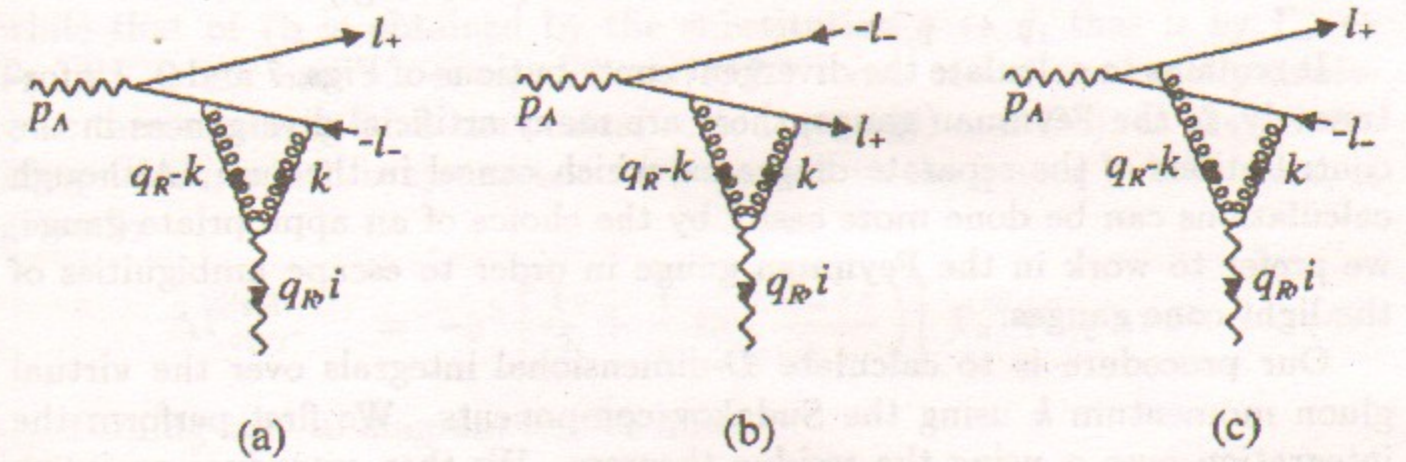


Figure 7: Diagrams containing the gluon-gluon-Reggeon vertex which contain the corrections to the  $\Gamma_{q\bar{q},\gamma^*}$  coming from Figs. 5 and 6.

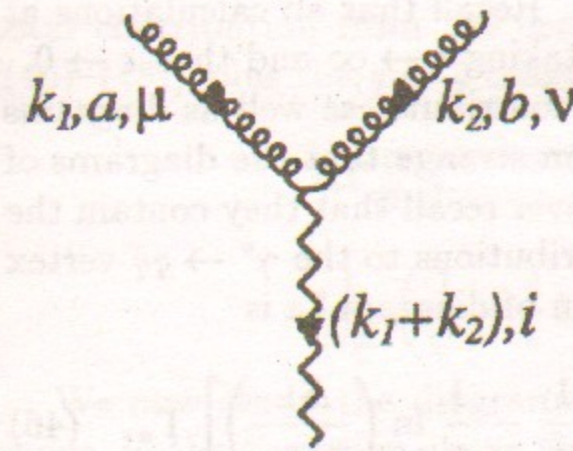


Figure 8: The gluon-gluon-Reggeon vertex of (41).



In addition to the two-gluon exchange contributions, we have also to include corrections to the  $\gamma^* \rightarrow q\bar{q}$  vertex coming from the diagrams of Fig. 9, as well as from the quark self-energy diagrams, and also from half of the self-energy contribution of the gluon of momentum  $q_R$ . The latter contribution is not infrared divergent and will not be discussed further.

### 3.2 Loop diagrams within the produced $q\bar{q}$ pair

The infrared divergent contribution of the quark self-energy diagrams can be found as follows. First the self-energy of the internal fermion lines is not infrared divergent. For the external lines, in dimensional regularization, the ultraviolet and infrared divergences cancel. Therefore it is simplest to determine the infrared divergence by taking the ultraviolet divergence with the opposite sign. It gives

$$\Delta\Gamma_{q\bar{q},\gamma^*}^{i(\text{quark self-energy})} = \Gamma_{q\bar{q},\gamma^*}^{(0)i} \left( -\frac{\bar{g}^2}{\epsilon} \frac{C_F}{N_C} \right). \quad (45)$$

It remains to calculate the divergent contributions of Figs. 7 and 9. Unfortunately, in the Feynman gauge, there are many artificial divergences in the contributions of the separate diagrams, which cancel in the sum. Although calculations can be done more easily by the choice of an appropriate gauge, we prefer to work in the Feynman gauge in order to escape ambiguities of the light-cone gauges.

Our procedure is to calculate  $D$ -dimensional integrals over the virtual gluon momentum  $k$  using the Sudakov components. We first perform the integration over  $\alpha$  using the residue theorem. We then introduce an intermediate parameter  $x_0$  to consider the collinear singularities in the regions  $|\beta| < x_0$  and  $|\beta| > x_0$  separately. We take  $x_0$  small,  $x_0 \ll 1$ . We let it tend to zero but not before  $\epsilon \rightarrow 0$ , so that  $\epsilon \ln(1/x_0) \rightarrow 0$  as  $\epsilon \rightarrow 0$ . On the other hand we take  $\beta_0 \rightarrow 0$  before  $\epsilon \rightarrow 0$ . Recall that all calculations at next-to-leading order are performed by first taking  $s \rightarrow \infty$  and then  $\epsilon \rightarrow 0$ .

For  $|\beta| < x_0$  all three diagrams of Fig. 7 contribute, as well as diagrams a1 and b1 of Fig. 9. At first sight it may seem strange that the diagrams of Fig. 7 are divergent in the 'soft' region. However recall that they contain the gluon-gluon-Reggeon vertex and receive contributions to the  $\gamma^* \rightarrow q\bar{q}$  vertex from the diagrams of Fig. 5. The contribution of diagram 7a is

$$\Delta\Gamma_{q\bar{q},\gamma^*}^{(\text{soft } 7a)} = -\bar{g}^2 \left[ \frac{\Gamma^2(\epsilon)}{\Gamma(2\epsilon)} (q_R^2)^\epsilon \ln \frac{1}{\beta_0} - \frac{1}{\epsilon^2} - \frac{1}{\epsilon} \ln \left( \frac{\Delta_-}{x_0 x_-} \right) \right] \Gamma_a, \quad (46)$$

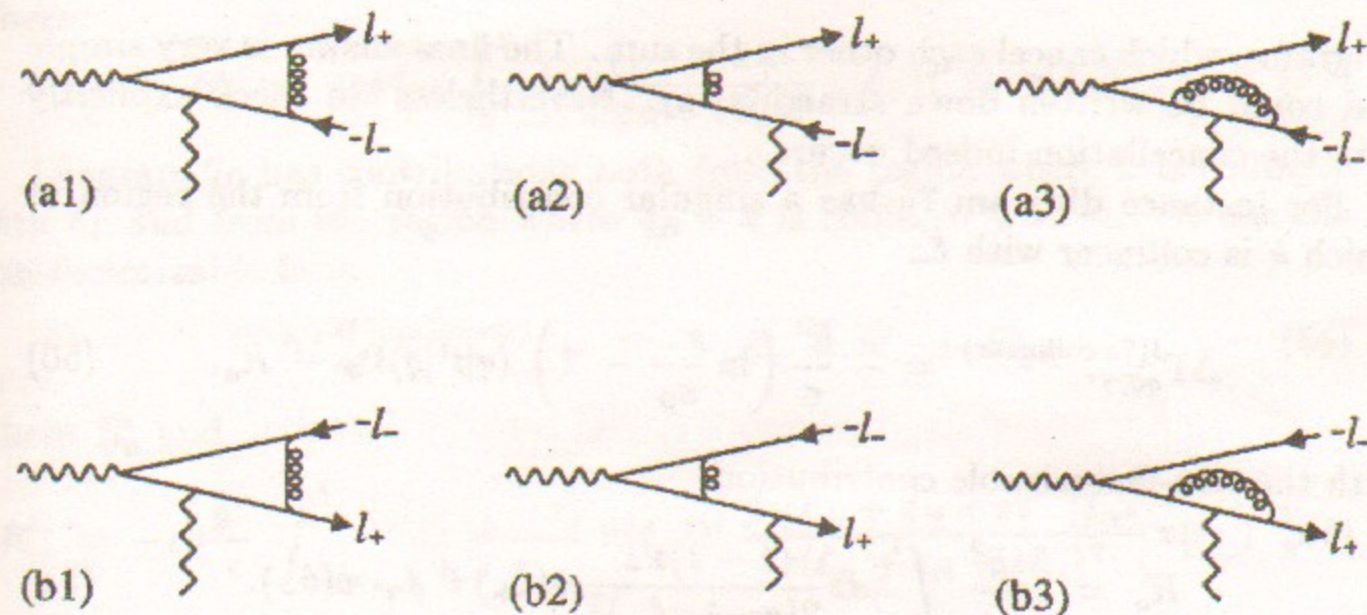


Figure 9: Loop diagrams within the produced  $q\bar{q}$  pair. The quark (antiquark) self-energy diagrams are not shown.

while that of 7b is obtained by the substitution  $q \leftrightarrow \bar{q}$ , that is by  $\Gamma_a \leftrightarrow \Gamma_b$ ,  $\Delta_- \leftrightarrow \Delta_+$  and  $x_- \leftrightarrow x_+$ . The  $\ln(1/\beta_0)$  terms cancel the exactly analogous terms coming from the central region, see (44) and (38), as they must. Diagram 7c, which is symmetric with respect to the  $q \leftrightarrow \bar{q}$  substitution, is given by

$$\Delta\Gamma_{q\bar{q},\gamma^*}^{(\text{soft } 7c)} = -\bar{g}^2 \left[ \frac{1}{\epsilon^2} + \frac{1}{\epsilon} \ln \left( \frac{\Delta_- x_0}{x_-} \right) \right] \Gamma_a + (q \leftrightarrow \bar{q}). \quad (47)$$

Turning now to diagram 9a1 we have

$$\Delta\Gamma_{q\bar{q},\gamma^*}^{(\text{soft } 9a1)} = \bar{g}^2 \frac{1}{N_C^2} \left[ \frac{1}{\epsilon^2} + \frac{1}{\epsilon} \ln \left( \frac{(\ell_+ + \ell_-)^2 x_0^2}{x_+ x_-} \right) \right] \Gamma_a, \quad (48)$$

while the contribution of 9b1 is obtained by the substitution  $q \leftrightarrow \bar{q}$ . The total contribution from the central region [(44), (38)] and the soft region [(46)–(48)], plus the  $q \leftrightarrow \bar{q}$  diagrams of 7b and 9b1] is

$$\Delta\Gamma_{q\bar{q},\gamma^*}^{i(\text{soft} + \text{central})} = -\bar{g}^2 \left[ \frac{1}{\epsilon^2} + \frac{1}{\epsilon} \ln(q_R^2 x_0^2) - \frac{1}{N_C^2} \left( \frac{1}{\epsilon^2} + \frac{1}{\epsilon} \ln \left( \frac{(\ell_+ + \ell_-)^2 x_0^2}{x_+ x_-} \right) \right) \right] \Gamma_{q\bar{q},\gamma^*}^{(0)i}. \quad (49)$$

We now study the diagrams with *collinear* singularities. As mentioned above, in the Feynman gauge there are artificial singularities in the separate



diagrams, which cancel each other in the sum. The final answer is very simple and could be written down straightaway. Nevertheless we check explicitly that the cancellation indeed occurs.

For instance diagram 7a has a singular contribution from the region in which  $k$  is collinear with  $\ell_-$

$$\Delta\Gamma_{q\bar{q},\gamma^*}^{i(7a \text{ collinear})} = -\frac{\bar{g}^2}{\epsilon} \left( \ln \frac{x_-}{x_0} - 1 \right) \langle q|t^i|\bar{q} \rangle \Gamma_a - R_a^i, \quad (50)$$

with the non-factorizable contribution

$$R_a^i = eg \frac{\bar{g}^2}{\epsilon} \int_0^1 dz \frac{(1-z)x_-}{2(q_R + z\ell_-)^2} \bar{u}(\ell_+) t^i \not{\ell}_+ \not{v}(\ell_-). \quad (51)$$

It is easy to understand the origin of such non-factorizable terms, and to follow their mutual cancellation using the gauge properties of the gluon vertices. The gluon-gluon-Reggeon vertex (41) gives

$$\gamma_{iab}^{\mu\nu}(k_1, k_2) k_2^\nu = -\frac{ig}{s} T_{ab}^i [k_1^2 p_2^\mu + (k_2 \cdot p_2) k_1^\mu], \quad (52)$$

since  $p_2 \cdot k_2 \simeq -p_2 \cdot k_1$  as the Reggeon momentum  $q_R = k_1 - k_2$  is almost transverse; thus  $p_2 \cdot q_R$  does not grow with  $s$ , whereas  $p_2 \cdot k_1$  and  $p_2 \cdot k_2$  are proportional to  $s$ . A vertex describing the interaction of a collinear gluon and a fermion gives us a gluon momentum which has to be contracted (via the gluon propagator) with another gluon vertex. For example, in the region where  $k$  and  $\ell_-$  are collinear,  $k \simeq -z\ell_-$ , the matrix element of diagram 7a contains the factor

$$(\not{\ell}_- + \not{k}) \gamma^\nu v(\ell_-) \simeq (1-z) \not{\ell}_- \gamma^\nu v(\ell_-) \simeq 2(1-z) \not{\ell}_- v(\ell_-) \simeq -2 \frac{(1-z)}{z} k^\nu v(\ell_-). \quad (53)$$

Now we use the gauge properties of the vertices. For diagram 7a we put  $k_2 = k$  and  $k_1 = q_R - k$  into the gluon-gluon-Reggeon vertex of (52). The first term gives a contribution proportional to  $\Gamma_a$ , and the second term the non-factorizable contribution  $R_a^i$  of (51), where we recognize the gluon propagator with momentum  $q_R - k$  with  $k = -z\ell_-$ .

The contribution of diagram 7b has a form analogous to (50), coming from the region where  $k$  is collinear with  $\ell_+$ ,

$$\Delta\Gamma_{q\bar{q},\gamma^*}^{i(7b \text{ collinear})} = -\frac{\bar{g}^2}{\epsilon} \left( \ln \frac{x_+}{x_0} - 1 \right) \langle q|t^i|\bar{q} \rangle \Gamma_b - R_b^i, \quad (54)$$

where

$$R_b^i \simeq -eg \frac{\bar{g}^2}{\epsilon} \int_0^1 dz \frac{(1-z)x_+}{2(q_R + z\ell_+)^2} \bar{u}(\ell_+) t^i \not{\ell}_+ \not{v}(\ell_-). \quad (55)$$

Diagram 7c has contributions both from the region where  $k$  is collinear with  $\ell_+$  and from the region where  $q_R - k$  is collinear with  $\ell_-$ . It has the non-factorizable form

$$\Delta\Gamma_{q\bar{q},\gamma^*}^{i(7c \text{ collinear})} = R_a^i + R_b^i + R_-^i + R_+^i, \quad (56)$$

where  $R_a^i$  and

$$R_-^i = -eg \frac{\bar{g}^2}{\epsilon} \int_{x_0/x_-}^1 dz \frac{(1-z)}{z} \bar{u}(\ell_+) t^i \frac{\not{p}_2(\not{\ell}_+ + \not{q}_R + z\ell_-) \not{\ell}_+}{s(\ell_+ + q_R + z\ell_-)^2} v(\ell_-) \quad (57)$$

come from the region where  $q_R - k$  is collinear with  $\ell_-$ . On the other hand  $R_b^i$  and

$$R_+^i = eg \frac{\bar{g}^2}{\epsilon} \int_{x_0/x_+}^1 dz \frac{(1-z)}{z} \bar{u}(\ell_+) t^i \frac{\not{\ell}_+ (\not{\ell}_- + \not{q}_R + z\ell_+) \not{p}_2}{s(\ell_- + q_R + z\ell_+)^2} v(\ell_-) \quad (58)$$

come from the region where  $k$  is collinear with  $\ell_+$ . We see that the contributions  $R_a^i$  and  $R_b^i$  cancel with the corresponding contributions of diagrams 7a and 7b respectively.

Contributions  $R_\pm^i$  cancel with analogous contributions from diagrams 9a1, a2 and 9b1, b2 respectively, which have the form

$$\Delta\Gamma_{q\bar{q},\gamma^*}^{i(9a1 \text{ collinear})} = -\frac{1}{N_C^2} R_+^i - R_+^i \quad (59)$$

$$\Delta\Gamma_{q\bar{q},\gamma^*}^{i(9a2)} = -\frac{\bar{g}^2}{\epsilon} \frac{2C_F}{N_C} \left( \ln \frac{x_+}{x_0} - 1 \right) \langle q|t^i|\bar{q} \rangle \Gamma_a - \frac{2C_F}{N_C} R_+^i \quad (60)$$

$$\Delta\Gamma_{q\bar{q},\gamma^*}^{i(9b1 \text{ collinear})} = -\frac{1}{N_C^2} R_-^i - R_-^i \quad (61)$$

$$\Delta\Gamma_{q\bar{q},\gamma^*}^{i(9b2)} = -\frac{\bar{g}^2}{\epsilon} \frac{2C_F}{N_C} \left( \ln \frac{x_-}{x_0} - 1 \right) \langle q|t^i|\bar{q} \rangle \Gamma_b - \frac{2C_F}{N_C} R_-^i, \quad (62)$$

where we have not used the 'collinear' superscript for those diagrams which do not have soft singularities. These contributions contain further artificial non-factorizable singularities

$$R_1^i = eg \frac{\bar{g}^2}{\epsilon} \frac{1}{N_C^2} \int_{x_0/x_-}^1 dz \frac{(1-z)}{z} \bar{u}(\ell_+) t^i \frac{\not{\ell}_+ (\not{q}_R + (1-z)\not{\ell}_-) \not{p}_2}{(q_R + (1-z)\ell_-)^2} v(\ell_-) \quad (63)$$



$$R_2^i = -eg \frac{\bar{g}^2}{\epsilon} \frac{1}{N_C^2} \int_{x_0/x_+}^1 dz \frac{(1-z)}{z} \bar{u}(\ell_+) t^i \frac{\not{p}_2(\not{q}_R + (1-z)\not{\ell}_+)\not{\ell}_+ \gamma^* v(\ell_-). \quad (64)$$

They in turn cancel with the contributions of diagrams 9a3, b3.

$$\Delta\Gamma_{q\bar{q},\gamma^*}^{i(9a3)} = \frac{\bar{g}^2}{N_C^2 \epsilon} \left( \ln \frac{x_-}{x_0} - 1 \right) \langle q|t^i|\bar{q} \rangle \Gamma_a + R_1^i$$

$$\Delta\Gamma_{q\bar{q},\gamma^*}^{i(9b3)} = \frac{\bar{g}^2}{N_C^2 \epsilon} \left( \ln \frac{x_+}{x_0} - 1 \right) \langle q|t^i|\bar{q} \rangle \Gamma_b + R_2^i.$$

Taking the sum of all these contributions and adding to it the quark self-energy contribution (45), which we may call collinear as well, we obtain

$$\Delta\Gamma_{q\bar{q},\gamma^*}^{i(\text{collinear})} = -\frac{2\bar{g}^2}{\epsilon} \frac{C_F}{N_C} \left( \ln \frac{x_+ x_-}{x_0^2} - \frac{3}{2} \right) \Gamma_{q\bar{q},\gamma^*}^{(0)i}. \quad (65)$$

As mentioned earlier, this answer could have been written 'by hand', since the expression in brackets is easily recognized as arising from the quark splitting function

$$\left( \int_{x_0/x_+}^1 + \int_{x_0/x_-}^1 \right) dz P_{gq}(z) = \left( \int_{x_0/x_+}^1 + \int_{x_0/x_-}^1 \right) dz \frac{1}{2z} (1 + (1-z)^2).$$

We see that the verification of (65) in the Feynman gauge is complicated by the presence of spurious singular terms which mutually cancel. Nevertheless we prefer to use this gauge so as to minimize the possible error in the subsequent evaluation of the non-singular terms.

### 3.3 Total singular virtual contribution

The total singular part of the virtual correction to the Reggeon vertex for  $\gamma^* \rightarrow q\bar{q}$  is given by the sum of the 'soft + central' contribution of (49) and the 'collinear' contribution of (65). It is

$$\Delta\Gamma_{q\bar{q},\gamma^*}^i = -\bar{g}^2 \left[ \frac{1}{\epsilon^2} + \frac{1}{\epsilon} \left( \ln(x_+ x_- q_R^2) - \frac{3}{2} \right) - \frac{1}{N_C^2} \left( \frac{1}{\epsilon^2} + \frac{1}{\epsilon} \left\{ \ln(\ell_+ + \ell_-)^2 - \frac{3}{2} \right\} \right) \right] \Gamma_{q\bar{q},\gamma^*}^{(0)i}. \quad (66)$$

## 4 Real gluon emission

Now we consider the contribution to the photon impact factor from the quark-antiquark-gluon intermediate state. First, we have to find the  $\gamma^* R \rightarrow q\bar{q}g$  effective vertex. In principle, we could use the same approach as for the  $\gamma^* R \rightarrow q\bar{q}$  vertex. Namely, we could calculate the amplitude for the conversion of a virtual photon into a  $q\bar{q}g$  state in the high energy collision of the photon with a quark, take the part of this amplitude with a colour-octet state in the  $t$  channel and determine the  $\gamma^* R \rightarrow q\bar{q}g$  vertex by comparison of this part with the Regge form (5). Since we need the vertex only in the Born approximation, it is sufficient to calculate the conversion amplitude in the same approximation and to take the Regge form in the lowest approximation in the coupling constant.

The expression for the vertex can be obtained immediately, if we represent it by the diagrams of Fig. 10 with the vertex factor  $igt^i \not{p}_2/s$  for the interaction of the Reggeon with quarks, and by the vertex factor  $\gamma_{iab}^{\mu\nu}$  (41) for the interaction of the Reggeon with gluons. It is straightforward to check that this direct calculation gives exactly the same  $\gamma^* R \rightarrow q\bar{q}g$  vertex as the method described above.

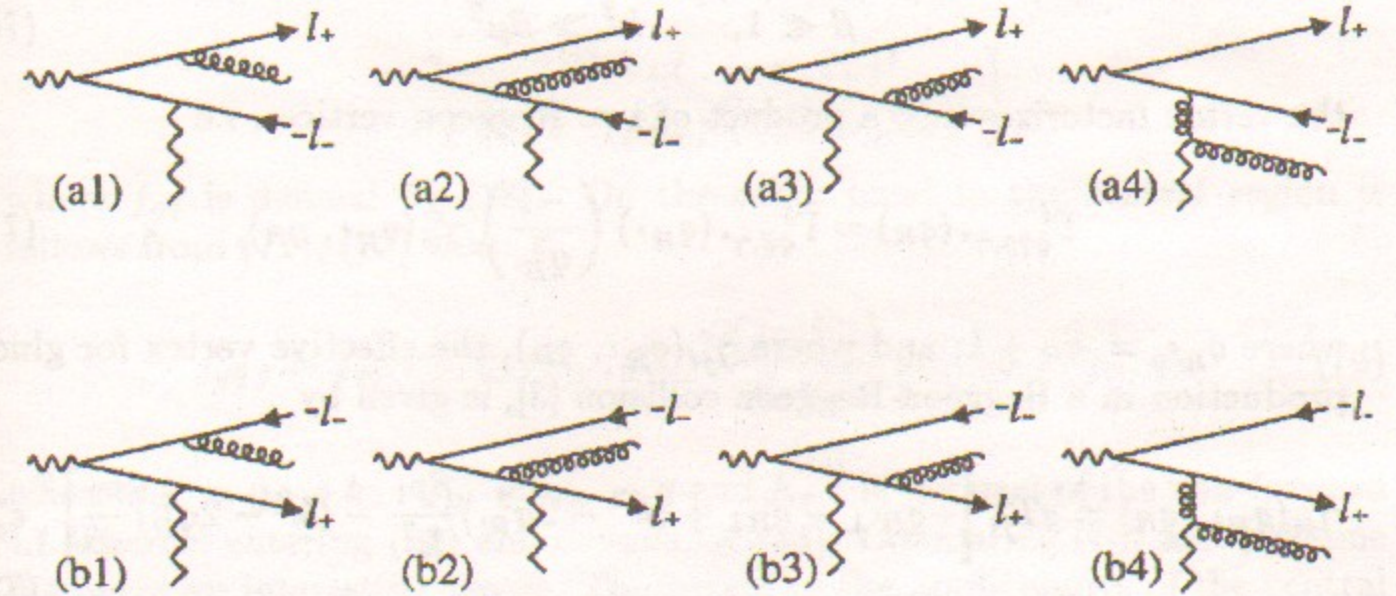


Figure 10: The real gluon emission diagrams from the  $\Gamma_{q\bar{q},\gamma^*}$  vertex.

In the following we denote the momentum, polarisation vector and colour index of the emitted gluon by  $k, e$  and  $c$  respectively. The Sudakov decom-



position is

$$k = \beta p_1 + \frac{k^2}{s\beta} p_2 + k_\perp, \quad k^2 \equiv -k_\perp^2. \quad (67)$$

The vertex  $\gamma^* R \rightarrow q\bar{q}g$  has the following properties.

1. In the 'soft' region

$$\beta \ll 1, \quad k^2 \ll \mu^2, \quad (68)$$

the vertex is given by the formula for accompanying soft bremsstrahlung, i.e.

$$\begin{aligned} \Gamma_{q\bar{q}g,\gamma^*}^i(q_R) = & \Gamma_{q\bar{q},\gamma^*}(q_R)g \left[ \left( \frac{\ell_+}{k.\ell_+} - \frac{p_2}{k.p_2} \right)^\mu \langle q|t^c t^i|\bar{q} \rangle \right. \\ & \left. - \left( \frac{\ell_-}{k.\ell_-} - \frac{p_2}{k.p_2} \right)^\mu \langle q|t^i t^c|\bar{q} \rangle \right] e_\mu^*. \end{aligned} \quad (69)$$

2. In the 'central' region

$$\beta \ll 1, \quad k^2 \gg \beta\mu^2, \quad (70)$$

the vertex factorizes into a product of two Reggeon vertices, i.e.

$$\Gamma_{q\bar{q}g,\gamma^*}^i(q_R) = \Gamma_{q\bar{q},\gamma^*}^j(q_{R'}) \left( \frac{-1}{q_{R'}^2} \right) \gamma_{ji}^c(q_{R'}, q_R), \quad (71)$$

where  $q_{R'} = q_R + k$ , and where  $\gamma_{ji}^c(q_{R'}, q_R)$ , the effective vertex for gluon production in a Reggeon-Reggeon collision [3], is given by

$$\gamma_{ji}^c(q_{R'}, q_R) = gT_{ji}^c \left[ -q_{R'\perp} - q_{R\perp} + (k^2 - 2q_{R'}^2) \frac{\beta p_1}{k^2} - (k^2 - 2q_R^2) \frac{p_2}{s\beta} \right]^\mu e_\mu^*. \quad (72)$$

Note that in (4) the gluon momentum is neglected in the vertex  $\Gamma_{q\bar{q},\gamma^*}$ . The neglect is valid in the whole region (68), not only when  $2(k.\ell_\pm) \ll \mu^2$ , (i.e. when  $k^2 \ll \beta\mu^2$ ) where it is obviously true. In fact, it is a consequence of Gribov's theorem [18] concerning the region of applicability of formulas for accompanying soft bremsstrahlung. Thus the factorization (4) in the region (68) has a general nature. The same can be said about (71). This equation was also checked by direct calculation; but, in fact, it also has quite a general nature and is connected with gluon Reggeization in QCD.

The important point is that the soft (68) and central (70) regions overlap and cover the entire region  $\beta < x_0$  with  $x_0 \ll 1$ . Let us denote

$$\frac{1}{\sqrt{N_C^2 - 1}} \sum_{\{q\bar{q}g\}} \Gamma_{q\bar{q}g,\gamma^*}^{(0)i}(q_R) \Gamma_{q\bar{q}g,\gamma^*}^{(0)i}(q_R')^* = f_{q\bar{q}g}, \quad (73)$$

c.f. (18). The contribution of the  $q\bar{q}g$  intermediate state to the impact factor is given by the integral of the function  $f_{q\bar{q}g}$  over

$$\begin{aligned} \frac{dM_{q\bar{q}g}^2}{2\pi} d\rho_{q\bar{q}g} = & 2\delta(1 - x_+ - x_- - \beta)(2\pi)^{D-1} \delta(\ell_+ + \ell_- + q_R + k) \\ & \times \frac{dx_+}{2x_+} \frac{dx_-}{2x_-} \frac{d\beta}{2\beta} \frac{d^{D-2}\ell_+}{(2\pi)^{D-1}} \frac{d^{D-2}\ell_-}{(2\pi)^{D-1}} \frac{d^{D-2}k}{(2\pi)^{D-1}}, \end{aligned} \quad (74)$$

c.f. (19). In the soft region we find, using (4), that

$$\begin{aligned} f_{q\bar{q}g} = & f_{q\bar{q}}(x_\pm, \ell_\pm; q_R, q_R') \times 2g^2 N_C \left[ \frac{x_+^2}{(x_+k - \beta\ell_+)^2} + \frac{x_-^2}{(x_-k - \beta\ell_-)^2} \right. \\ & \left. - \frac{1}{N_C^2} \frac{\beta^2(x_+\ell_- - x_-\ell_+)^2}{(x_+k - \beta\ell_+)^2(x_-k - \beta\ell_-)^2} \right], \end{aligned} \quad (75)$$

where  $f_{q\bar{q}}$  is defined by (18). On the other hand in the central region it follows from (71), (72) that

$$f_{q\bar{q}g} = f_{q\bar{q}}(x_\pm, \ell_\pm; q_{R'}, q_R') \frac{2(2\pi)^{D-1}}{q_{R'}^2 q_R'^2} K_r^{(0)}(q_{R'}, q_R; q), \quad (76)$$

where  $q_{R'} = q_R + k$ ;  $q_R' = q_{R'} - q$  and  $K_r^{(0)}$  is the part of the non-forward LLA kernel entering (22) and defined by (23). Comparing (75) and (76) one discovers an interesting result. The region of the applicability of the central form (76) for  $f_{q\bar{q}g}$  is larger than (70) and, in fact, is given by

$$\beta \ll 1, \quad k^2 \gg \beta^2\mu^2. \quad (77)$$

It is convenient to consider the contribution of the central region together with the subtraction term in (22). This term has two types of infrared singularities: the singularities contained in the trajectory function  $\omega(t)$ , and the singularities coming from the integration over  $q_{R'}$ . Owing to properties (21) of the impact factor, the latter singularities are only due to the singular behaviour of the real part of  $K_r^{(0)}(q_{R'}, q_R; q)$  at  $q_{R'} - q_R = k = 0$ . It is



useful to note that in (22)  $\ln(s_0)$  appears as a factor of the total non-forward BFKL kernel,

$$K(\mathbf{q}_{R'}, \mathbf{q}_R; \mathbf{q}) = \mathbf{q}_R^2 \mathbf{q}'_R{}^2 \delta(\mathbf{q}_{R'} - \mathbf{q}_R) (\omega(t_R) + \omega(t'_R)) + K_r(\mathbf{q}_{R'}, \mathbf{q}_R; \mathbf{q}), \quad (78)$$

taken in the Born approximation. Since the total kernel is infrared safe, the infrared singularities do not depend on the value of  $s_0$ , so that we can take any suitable choice of  $s_0$  to analyse them. It is convenient to take  $s_0$  sufficiently large so that  $s_0 \gg \mu^2$ , but such that at the same time it satisfies  $s_0 \ll \mu^2/x_0^2$ .

Then we can evaluate the integral over  $f_{q\bar{q}g}$  in the region  $\beta \leq x_0$  as the sum of two subregions, in the first (second) of which  $k^2$  is less (larger) than  $\beta^2 s_0$ . The contribution of the first region can be calculated with the help of (75). Its singular part is

$$\int d\Phi_{\gamma^*, \gamma^*}^{(0)}(\mathbf{q}_R, \mathbf{q}) 2\bar{g}^2 \left[ \frac{1}{\epsilon^2} + \frac{1}{\epsilon} \ln(x_0^2 s_0) - \frac{1}{N_C^2} \left\{ \frac{1}{\epsilon^2} + \frac{1}{\epsilon} \ln \left( \frac{x_0^2 (\ell_- + \ell_+)^2}{x_+ x_-} \right) \right\} \right], \quad (79)$$

where

$$d\Phi_{\gamma^*, \gamma^*}^{(0)}(\mathbf{q}_R, \mathbf{q}) = f_{q\bar{q}}(x_\pm, \ell_\pm; \mathbf{q}_R, \mathbf{q}'_R) \frac{dM_{q\bar{q}}^2}{2\pi} d\rho_{q\bar{q}} \quad (80)$$

with the function  $f_{q\bar{q}}$  defined in (18) and the phase space element in (19), so that

$$\int d\Phi_{\gamma^*, \gamma^*}^{(0)}(\mathbf{q}_R, \mathbf{q}) = \Phi_{\gamma^*, \gamma^*}^{(0)}(\mathbf{q}_R, \mathbf{q}), \quad (81)$$

see (7) and (18). The contribution of the second region can be calculated with the help of (76). As already mentioned, it is convenient to consider this contribution together with the subtraction term in (22). Our choice of  $s_0$  makes such a consideration especially convenient because of the total cancellation of the singular part of this contribution with the part of the subtraction term involving  $K_r^{(0)}$ . So, the singular contribution from the second region and the subtraction term is simply

$$\Phi_{\gamma^*, \gamma^*}^{(0)}(\mathbf{q}_R, \mathbf{q}) \frac{\bar{g}^2}{\epsilon} \ln \left( \frac{\mathbf{q}_R^2 \mathbf{q}'_R{}^2}{s_0^2} \right). \quad (82)$$

The dependence on  $s_0$  vanishes in the sum of (79) and (82), as it must.

It remains to consider the singular contributions from the region  $\beta \geq x_0$ . These contributions have a collinear nature. For real emission we can use, without uncertainty, a physical gauge. In such a gauge, the  $\gamma^* R \rightarrow q\bar{q}g$  vertex

in the region of quasi-collinearity of the gluon and the quark (antiquark) momenta is given by the diagrams with a gluon line attached to the external quark (antiquark) line, Fig. 10a1, b1 (Fig. 10a3, b3). They can be easily calculated by the quasi-real electron method [19]. In this way the singular contribution from the region  $\beta \geq x_0$  is found to be

$$\int d\Phi_{\gamma^*, \gamma^*}^{(0)}(\mathbf{q}_R, \mathbf{q}) \frac{\bar{g}^2 2C_F}{\epsilon N_C} \left[ \left( \int_{x_0/x_+}^1 + \int_{x_0/x_-}^1 \right) \frac{dz}{z} (1 + (1-z)^2) \right] \\ = \int d\Phi_{\gamma^*, \gamma^*}^{(0)}(\mathbf{q}_R, \mathbf{q}) \frac{\bar{g}^2 2C_F}{\epsilon N_C} \left[ 2 \ln \left( \frac{x_+ x_-}{x_0^2} \right) - 3 \right]. \quad (83)$$

This completes the study of the real gluon emission contribution to the photon impact factor. The singular parts of this contribution together with the subtraction term in eq. (22) are given by (79), (82) and (83).

## 5 Cancellation of the infrared singularities

Let us denote the singular part of the virtual photon impact factor as the sum

$$\Phi_{\gamma^*, \gamma^*}(\mathbf{q}_R, \mathbf{q})_{\text{singular}} \quad (84)$$

$$= \int d\Phi_{\gamma^*, \gamma^*}^{(0)}(\mathbf{q}_R, \mathbf{q}) \left[ \delta_{\text{virtual}}^{\text{soft+central}} + \delta_{\text{virtual}}^{\text{collinear}} + \delta_{\text{real}}^{\text{soft}} + \delta_{\text{real}}^{\text{central}} + \delta_{\text{real}}^{\text{collinear}} \right].$$

Here the first two terms in the square brackets are the singular parts connected with the virtual corrections to the  $\gamma^* R \rightarrow q\bar{q}$  vertex and coming from the central and soft regions (49) and the collinear regions (65)

$$\delta_{\text{virtual}}^{\text{soft+central}} = -\bar{g}^2 \left[ \frac{2}{\epsilon^2} + \frac{1}{\epsilon} \ln(x_0^4 \mathbf{q}_R^2 \mathbf{q}'_R{}^2) - \frac{2}{N_C^2} \left( \frac{1}{\epsilon^2} + \frac{1}{\epsilon} \ln \left( \frac{x_0^2 (\ell_- + \ell_+)^2}{x_+ x_-} \right) \right) \right]. \quad (85)$$

$$\delta_{\text{virtual}}^{\text{collinear}} = -\frac{\bar{g}^2 2C_F}{\epsilon N_C} \left[ 2 \ln \left( \frac{x_+ x_-}{x_0^2} \right) - 3 \right]. \quad (86)$$

The next three terms are the singular parts of the contribution of the real gluon emission taken together with the subtraction term in (22). They are given by (79), (82) and (83)

$$\delta_{\text{real}}^{\text{soft}} = 2\bar{g}^2 \left[ \frac{1}{\epsilon^2} + \frac{1}{\epsilon} \ln(x_0^2 s_0) - \frac{1}{N_C^2} \left( \frac{1}{\epsilon^2} + \frac{1}{\epsilon} \ln \left( \frac{x_0^2 (\ell_- + \ell_+)^2}{x_+ x_-} \right) \right) \right], \quad (87)$$



$$\delta_{\text{real}}^{\text{central}} = \frac{\bar{g}^2}{\epsilon} \ln \left( \frac{q_R^2 q_R'^2}{s_0^2} \right), \quad (88)$$

and

$$\delta_{\text{real}}^{\text{collinear}} = \frac{\bar{g}^2}{\epsilon} \frac{2C_F}{N_c} \left[ 2 \ln \left( \frac{x_+ x_-}{x_0^2} \right) - 3 \right]. \quad (89)$$

We see that the sum of the contributions (85)-(89) is zero. That is the impact factor is infrared safe.

## 6 Infrared safety of impact factors in the general case

In the preceding Sections we have explicitly calculated the infrared contributions to the impact factor of the virtual photon coming from various sources, and have demonstrated their cancellation. In this Section we present general arguments, applicable to any impact factor, to prove its infrared safety. These arguments are based on well known theorems [20] about the absence of infrared divergences in totally inclusive quantities. Though these theorems are commonly used for cross sections and for the imaginary parts of forward scattering amplitudes, they apply equally well to non-forward scattering.

Therefore we could be sure of the infrared safety of the impact factors provided that Reggeons were a kind of off-mass-shell partons, described by some fields, and the impact factors were the imaginary parts of the amplitudes for the scattering of these 'partons' off particles. But this is not the case for several reasons. First, the impact factors contain the subtraction (see (22) where we have singularities due to the gluon trajectory function  $\omega(t)$  as well as arising from  $K_r^{(0)}$ ). Second, the region of integration over the phase space volume in (22) is restricted by a theta-function. And finally, the Reggeon-particle vertices  $\Gamma^i$  in (22) are not true field theory amplitudes.

The first two reasons are evident and do not need further explanation. Let us amplify the third reason. We noted that at the Born level the vertices  $\gamma^* R \rightarrow q\bar{q}$  and  $\gamma^* R \rightarrow q\bar{q}g$  are given by Feynman diagrams. It means, that these vertices appear as amplitudes of the effective field theory [16]. An analogous statement is applicable in the general case, but it is only valid in the Born approximation. Recall that the corrections to the  $\gamma^* R \rightarrow q\bar{q}$  vertex consist of two parts. One contribution, which comes from the central region of virtual gluon momenta (29), is given by (39) and is universal, i.e. process

independent. The other contribution, which comes from the  $A$ -region, is given by Feynman diagrams of the effective field theory with the restriction  $|\beta| \geq \beta_0$  on the Sudakov parameters of the gluon momenta. This last statement again has a general nature, i.e. in the general case the one-loop corrections to Reggeon-particle vertices are given by the sum of the universal contribution (39) and a part given by the effective field theory with the restriction  $|\beta| \geq \beta_0$  on gluon momenta. We can apply arguments [20] about the absence of infrared divergences to the imaginary parts of Reggeon-particle scattering amplitudes in this theory. From the above discussion it is clear how impact factors differ from such imaginary parts. They differ by

- 1) the existence of the subtraction term;
- 2) the presence of the contribution of (virtual and real) gluons with  $|\beta| \leq \beta_0$ ;
- 3) the limitation of the integration region over the phase space of the produced particles.

So, to be convinced that the impact factors are indeed infrared safe, we need to check the cancellation of the infrared contributions to the impact factor coming from these three sources.

It is convenient to use a notation analogous to (84) for the singular part of the next-to-leading correction to the impact factor

$$\Phi_{A'A}(q_R, q)_{\text{singular}} = \int d\Phi_{A'A}^{(0)}(q_R, q) [\delta_1 + \delta_2^{\text{virtual}} + \delta_2^{\text{real}} + \delta_3]. \quad (90)$$

Then, taking into account the properties (21) of the impact factors for colourless objects, we obtain from (22)-(25)

$$\begin{aligned} \delta_1 = & -\frac{1}{2} \left[ \int \frac{d^{D-2}k}{k^2} \frac{2g^2 N_C}{(2\pi)^{D-1}} \ln \left( \frac{s_\Lambda^2}{k^2 s_0} \right) + \omega(t_R) \ln \left( \frac{q_R^2}{s_0} \right) \right. \\ & \left. + \omega(t'_R) \ln \left( \frac{q_R'^2}{s_0} \right) \right]_{\text{singular}} = -\bar{g}^2 \left( \frac{2}{\epsilon^2} + \frac{1}{\epsilon} \ln \left( \frac{s_\Lambda^4}{q_R'^2 q_R^2} \right) \right). \end{aligned} \quad (91)$$

Recall from Section 3 that the contribution of virtual gluons with  $|\beta| \leq \beta_0$  is universal. It gives the correction (44) to Born vertex. Therefore, we obtain

$$\delta_2^{\text{virtual}} = -\bar{g}^2 \left( \frac{2}{\epsilon^2} + \frac{4}{\epsilon} \ln \beta_0 + \frac{1}{\epsilon} \ln (q_R'^2 q_R^2) \right). \quad (92)$$



It is appropriate to consider the contribution of real gluons with  $|\beta| \leq \beta_0$  together with the limitation  $M_a^2 \leq s_\Lambda$  of the integration region over the phase space of the produced partons in (22). This limitation does not play any role in the LLA, and becomes important only for gluon emission. Thus, in fact it is a limitation on the phase space of the emitted gluon to the region

$$\frac{k^2}{\beta} \leq s_\Lambda.$$

Recall that we take limit  $\beta_0 \rightarrow 0$  before  $\epsilon \rightarrow 0$ , so that for the calculation of the contribution of real gluons with  $|\beta| \leq \beta_0$  we can use the multi-Regge factorisation formula analogous to (76). Therefore we obtain

$$\begin{aligned} \delta_2^{\text{real}} + \delta_3 &= \frac{4g^2 N_C}{(2\pi)^{D-1}} \left[ \int \frac{d^{D-2}k}{k^2} \int_{k^2/s_\Lambda}^{\beta_0} \frac{d\beta}{2\beta} \right]_{\text{singular}} \\ &= 4\bar{g}^2 \left( \frac{1}{\epsilon^2} + \frac{1}{\epsilon} \ln(s_\Lambda \beta_0) \right). \end{aligned} \quad (93)$$

We see that the sum of (91)-(93) is zero, which means that we have verified the infrared safety of impact factors in general.

## 7 Discussion

In this paper we have investigated, to the next-to-leading order accuracy, the infrared properties of impact factors appearing in the BFKL description of small  $x$  processes. We have shown, by explicit calculation, the cancellation of the infrared singularities in the impact factor of the virtual photon. The virtual photon impact factor was considered because of the importance of corrections to LLA for diffractive  $q\bar{q}$  electroproduction and because of the possibility of calculating this impact factor in perturbation theory for large enough photon virtuality. We also presented a general proof of the infrared safety of the impact factors describing the transitions between colourless particles.

We have considered impact factors in the general case of non-forward scattering and have used the definition of impact factors given in [6, 8]. These impact factors are defined for the case when the energy scale  $s_0$  (in the Mellin transform factor  $(s/s_0)^\omega$  in (2)) is a constant independent of the integration variables (the Reggeon "masses"). One may prefer to use a scale which is

dependent on these variables. (For instance in the particular case of forward scattering, i.e. for calculation of cross sections, the scale  $\sqrt{q_1^2 q_2^2}$  was used in [4]). It was shown in [15] that to the NLA accuracy one can indeed change the scale  $s_0$  in (2) for any factorizable scale  $f_1 f_2$ , with  $f_i$  depending on  $q_i$  (and on  $q$ ), without changing the Green function, provided that the impact factors are also changed according to

$$\begin{aligned} \Phi_{A'A}(q_R, q; s_0) &\rightarrow \Phi_{A'A}(q_R, q; s_0) \\ &+ \frac{1}{2} \int \frac{d^{D-2}q_{R'}}{q_{R'}^2 q_{R'}'^2} \Phi_{A'A}^{(0)}(q_{R'}, q) K^{(0)}(q_{R'}, q_R; q) \ln \left( \frac{f_R}{s_0} \right), \end{aligned} \quad (94)$$

where  $K^{(0)}$  is the total non-forward LLA kernel,

$$K^{(0)}(q_{R'}, q_R; q) = K_r^{(0)}(q_{R'}, q_R; q) + q_{R'}^2 q_R^2 \delta(q_R - q_{R'}) (\omega(t_R) + \omega(t'_R)). \quad (95)$$

$K_r^{(0)}$  is the part of the LLA kernel related to real gluon production, (23), and  $\omega(t)$  is the gluon Regge trajectory. The properties of the impact factors (20) and the infrared safety of the total kernel (due to cancellation of the infrared singularities connected with  $K_r^{(0)}$  and with the gluon trajectory) guarantees that the transformation (94) does not change the infrared properties of the impact factors.

We emphasize that the above definitions differ from those introduced, for the case of the forward scattering, in [13] and used in [5] and in [14], where impact factors of partons (quarks and gluons) were calculated for a colour singlet state in the  $t$  channel. The definition advocated in these papers is based on "the requirement that the subtracted leading term should satisfy at finite energies for the impact factors to be well defined (e.g., without spurious infrared divergencies)" [14]. In order to fulfil this requirement additional operator factors  $H_L, H_R$  were introduced [5], [14] in the Green function  $G_\omega$ . In our opinion, the only physical requirement is the absence of infrared singularities in the impact factors of colourless objects, and we have explicitly demonstrated here that our definition of the impact factors fulfills this important requirement.

**Acknowledgements.** We thank the Royal Society and INTAS (95-311) for financial support.



## References

- [1] A.M. Cooper-Sarkar, R.C.E. Devenish and A. De Roeck, *Int. J. Mod. Phys. A* **13** (1998) 3385, and references therein.
- [2] See, for example, A.D. Martin, M.G. Ryskin and T. Teubner, *Phys. Rev. D* **55** (1997) 4329.
- [3] V.S. Fadin, E.A. Kuraev and L.N. Lipatov, *Phys. Lett. B* **60** (1975) 50; E.A. Kuraev, L.N. Lipatov and V.S. Fadin, *Z. Eksp. Teor. Fiz.* **71** (1976) 840 [*Sov. Phys. JETP* **44** (1976) 443]; **72** (1977) 377 [**45** (1977) 199]; Ya.Ya. Balitski and L.N. Lipatov, *Sov. J. Nucl. Phys.* **28** (1978) 822.
- [4] V.S. Fadin and L.N. Lipatov, *Phys. Lett. B* **429** (1998) 127.
- [5] M. Ciafaloni and G. Camici, *Phys. Lett. B* **430** (1998) 349.
- [6] V.S. Fadin and R. Fiore, *Phys. Lett. B* **440** (1998) 359.
- [7] D.A. Ross, *Phys. Lett. B* **431** (1998) 161; Yu.V. Kovchegov, A.H. Mueller, *Phys. Lett. B* **439** (1998) 423; J. Blumlein, A. Vogt, *Phys. Rev. D* **57** (1998) 1; *Phys. Rev. D* **58** (1998) 014020; J. Blumlein, V. Ravindran, W.L. van Neerven, A. Vogt, preprint DESY-98-036 ([hep-ph/9806368](http://hep-ph/9806368)); E.M. Levin, preprint TAUP 2501-98 ([hep-ph/9806228](http://hep-ph/9806228)); N. Armesto, J. Bartels, M.A. Braun, *Phys. Lett. B* **442** (1998) 459; G.P. Salam, *JHEP* **8907** (1998) 19.
- [8] V.S. Fadin, preprint Budker INP 98-55; [hep-ph/9807528](http://hep-ph/9807528), to be published in Proceedings of the International Conference "LISHEP98", 14-20 February, 1998, Rio de Janeiro, Brazil.
- [9] L.N. Lipatov and V.S. Fadin, *Z. Eksp. Teor. Fiz. Pis'ma* **49** (1989) 311 [*Sov. Phys. JETP Lett.* **49** (1989) 352]; *Yad. Fiz.* **50** (1989) 1141 [*Sov. J. Nucl. Phys.* **50** (1989) 712]; V.S. Fadin and L.N. Lipatov, *Nucl. Phys. B* **406** (1993) 259; V.S. Fadin, R. Fiore and A. Quartarolo, *Phys. Rev. D* **50** (1994) 5893; V.S. Fadin, R. Fiore and M.I. Kotsky, *Phys. Lett. B* **389** (1996) 737; V.S. Fadin, M.I. Kotsky and L.N. Lipatov, *Phys. Lett. B* **415** (1997) 97; *Yad. Fiz.* **61**(6) (1998) 716; V.S. Fadin, R. Fiore, A. Flachi and M.I. Kotsky, *Phys. Lett. B* **422** (1998) 28.
- [10] V.S. Fadin, R. Fiore and A. Quartarolo, *Phys. Rev. D* **50** (1994) 2265; V.S. Fadin, R. Fiore and M.I. Kotsky, *Phys. Lett. B* **359** (1995) 181.
- [11] V.S. Fadin, R. Fiore and M.I. Kotsky, *Phys. Lett. B* **387** (1996) 593.
- [12] S. Catani, M. Ciafaloni and F. Hautmann, *Phys. Lett. B* **242** (1990) 97; *Nucl. Phys. B* **366** (1991) 135; G. Camici and M. Ciafaloni, *Phys. Lett. B* **386** (1996) 341; *Nucl. Phys. B* **496** (1997) 305.
- [13] M. Ciafaloni, *Phys. Lett. B* **429** (1998) 363.
- [14] M. Ciafaloni and D. Colferai, *Nucl. Phys. B* **538** (1999) 187.
- [15] V.S. Fadin, in: Proceedings of the 6-th International Workshop on Deep Inelastic Scattering and QCD (DIS 98); editors: G.H. Coremans, R. Roosen; World Scientific, 1998; pp. 747-751; [hep-ph/9807527](http://hep-ph/9807527).
- [16] L.N. Lipatov, *Nucl. Phys. B* **452** (1995) 369; *Physics Reports* **286** (1997) 132.
- [17] V.N. Gribov, L.N. Lipatov and G.V. Frolov, *Phys. Lett. B* **31B** (1970) 34; *Yad. Fiz.* **12** (1970) 994 [*Sov. J. Nucl. Phys.* **12** (1971) 543]; H. Cheng and T.T. Wu, *Phys. Rev. D* **1** (1970) 2775.
- [18] V.N. Gribov, *Yad. Fiz.* **5** (1967) 399.
- [19] V.N. Baier, V.S. Fadin and V.A. Khoze, *Nucl. Phys. B* **65** (1973) 381.
- [20] F. Bloch and A. Nordsieck, *Phys. Rev.* **52** (1937) 54; D.R. Yennie, S.C. Frautschi and H. Suura, *Ann. Phys. (NY)* **13** (1961) 379; T. Kinoshita, *J. Math. Phys.* **3** (1962) 650; T.D. Lee and M. Nauenberg, *Phys. Rev. B* **133** (1964) 1549.



*V.S. Fadin and A.D. Martin*

**Infrared safety of impact factors  
for colourless particle interactions**

*В.С. Фадин, А.Д. Мартин*

**Инфракрасная стабильность  
импакт факторов бесцветных частиц**

Budker INP 99-38

Ответственный за выпуск А.М. Кудрявцев  
Работа поступила 28.04.1999 г.

---

Сдано в набор 30.04.1999 г.  
Подписано в печать 30.04.1999 г.  
Формат бумаги 60×90 1/16 Объем 1.8 печ.л., 1.5 уч.-изд.л.  
Тираж 100 экз. Бесплатно. Заказ № 38

---

Обработано на IBM PC и отпечатано на  
ротапринтере ИЯФ им. Г.И. Будкера СО РАН  
Новосибирск, 630090, пр. академика Лаврентьева, 11.